# NUTRIENT DYNAMICS OF FRESHWATER ESTUARINE SEDIMENTS DISTURBED BY DREDGING

by

Ryan A. J. Roekle

A Thesis Submitted in

Partial Fulfillment of the

Requirements for the Degree of

Master of Science

in Freshwater Sciences and Technology

at

The University of Wisconsin-Milwaukee

August 2023

ABSTRACT

NUTRIENT DYNAMICS OF FRESHWATER ESTUARINE SEDIMENTS DISTURBED BY DREDGING

by

Ryan A. J. Roekle

The University of Wisconsin-Milwaukee, 2023
Under the Supervision of Dr. Russell Cuhel

This study examined the nutrient environment of sediments in the Milwaukee River estuary and the dynamics of those nutrients during simulated disturbance experiments within the context of large-scale dredging remediation. Surface sediments were collected from throughout the Milwaukee estuary (including river, harbor, and nearshore stations) by PONAR, centrifuged to separate porewater (interstitial water) from solid material, and filtered to further isolate and stabilize dissolved material. Porewaters were analyzed for dissolved nutrients including ammoniacal nitrogen (AN), nitrate, nitrite, and soluble reactive phosphorus (SRP). Surface sediment porewaters within the estuary were often highly enriched in AN and SRP, which were often 10-2000x more concentrated in estuarine surface sediment porewaters than their overlying water columns, with AN ranging from 150-2000 µM and SRP ranging from 0.1-70 µM. Nitrate concentrations in surface sediment porewaters were strongly depleted relative to overlying waters—between 0.01-0.40x. Simulated disturbance experiments designed to approximate dredging-induced disturbances were performed on sediment samples, which involved continuously mixing whole sediments with filtered harbor water. In these experiments, more AN and SRP were released into the receiving waters than was expected based on the concentrations present in the sediment porewaters initially, with AN reaching concentrations 4-10x higher than

expected within 4-5 hours. These dynamics suggest organic decomposition within the first 4-5 hours after the initial disturbance while the sediments were still resuspended. In most samples, AN was depleted to very low concentrations within 2 days of the initial disturbance. Nitrite, the intermediate product of complete ammonia oxidation, rose to moderate concentrations before also being depleted to low concentrations for the remaining 1-3 weeks of the experiments. Nitrate, the end product of complete ammonia oxidation, rose gradually throughout the remaining weeks of the experiments to concentrations 1-25x higher than predicted. These dynamics strongly suggest nitrification. Soluble reactive phosphorus also reached concentrations 2-12x higher than predicted, rising quickly in the first 4-5 hours after mixing then more slowly over the following weeks. Alongside decomposition, this may also be the result of particulate inorganic phosphorus (PIP) dissolution due to acidification by nitrification. The concentrations and forms of eutrophicating nutrients released by dredge plumes or effluent discharged from confined disposal facilities are determined not only by the initial dissolved nutrient contents of sediment porewaters but by biogeochemical processes at the sediment-water interface such as those described here. The nature of these biogeochemical processes as they relate to dredging will influence the ecological effects of dredging on the surrounding environment.

# TABLE OF CONTENTS

# LIST OF FIGURES

# LIST OF TABLES

# LIST OF ABBREVIATIONS

| | |
|---|---|
| AOB | Ammonia-Oxidizing Bacteria |
| AN | Ammoniacal Nitrogen |
| AOC | Area of Concern |
| BUI | Beneficial Use Impairment |
| CDF | Confined Disposal Facility |
| DIC | Dissolved Inorganic Carbon |
| DIN | Dissolved Inorganic Nitrogen |
| DIP | Dissolved Inorganic Phosphorus |
| DON | Dissolved Organic Nitrogen |
| DMMF/DMDF | Dredged Material Management/Disposal Facility |
| DNRA | Dissimilatory Nitrate Reduction to Ammonium |
| FP | Filterable Phosphorus |
| MMSD | Milwaukee Metropolitan Sewerage District |
| NOB | Nitrite-Oxidizing Bacteria |
| NPOC | Non-Purgeable Organic Carbon |
| PES | Polyether Sulfone |
| PIP | Particulate Inorganic Phosphorus |
| POM | Particulate Organic Matter |
| SRP | Soluble Reactive Phosphorus |
| SWI | Sediment-Water Interface |
| TAN | Total Ammoniacal Nitrogen |

| | |
|---|---|
| TN | Total Nitrogen |
| USACE | United States Army Corps of Engineers |
| USEPA | United States Environmental Protection Agency |
| WDNR | Wisconsin Department of Natural Resources |

# ACKNOWLEDGEMENTS

My deepest gratitude and appreciation go to Dr. Russell Cuhel and Dr. Carmen Aguilar for jointly acting as my primary thesis advisors, PIs, mentors, and advocates since I began my work at the School of Freshwater Sciences as an undergraduate. I would also like to thank Dr. Jim Waples for serving on my committee and providing advice, as well as for being an outstanding professor. For their analytical and field work contributions, my thanks go to Sharon Zsebe, Tim Wahl, and Dr. John Ejnik. Additional thanks to Captain Max Morgan and the crew of the R/V Neeskay, and to my family. Funding for this study was provided by the UWM Office of Research through their 2022 Discovery and Innovation Grant (DIG) to Drs. Aguilar and Cuhel, the Mick A. Naulin Foundation, and the management district for the inland lake on which this project was originally conceived.

# 1 INTRODUCTION

## 1.1 Background

Chemical fluxes at the sediment-water interface play crucial roles in establishing the chemical environments of both sediments and their overlying water columns in freshwater systems. In part, sediments are assumed to be nutrient enriched compared to the corresponding water column due to the decomposition of organic material [Pettersson 1998, Zhong 2021]. Biogeochemical processes within sediments can transform nutrient composition [Boulton 2010, Zilius 2012, Nogaro 2014, Benelli 2017]. In enclosed or semi-enclosed bodies of water, such as lakes, bays, or wetlands, nutrient flux across the sediment-water interface (SWI) can account for a consequential fraction of the total nutrient load [Smolders 2006, Sugimoto 2014, Larson 2020, Moncelon 2021]. Disturbance of sediments by anthropogenic activities such as dredging or bottom-trawling can elevate chemical fluxes from sediments in aquatic environments by releasing sequestered nutrients *en masse* into the waters above [Windom 1975; Tramontano & Bohlen 1984; Lohrer & Wetz 2003; Warnken 2003]. Disturbances additionally can alter the biogeochemical processes that affect normal nutrient fluxes across the SWI more generally [Brooks & Edgington 1994, Bradshaw 2021, Zhong 2021]. With the release of nutrients into the water, in particular bioavailable nitrogen and phosphorus, comes the risk of triggering the formation of algal blooms, a phenomenon long associated with increased N and P loading into aquatic environments [D'Elia 1987, Nixon 1995, Carpenter 1998]. The possibility of triggering the growth of algal blooms fed by nutrients liberated from dredged sediments is of particular interest in Milwaukee given how valued the lower rivers and harbor are for recreation, transportation, and their influences on drinking water quality.

To date, most research on chemical repercussions of dredging has been conducted in nearshore marine or brackish estuarine environments surrounding human development projects (e.g. construction and maintenance of navigation channels) [Choppala 2018], or sediment resuspension in the context of bottom-trawling fisheries management [Warnken 2003, Bradshaw 2021]. Attempts to ascertain a universal consensus on chemical effects of dredging on surrounding waters have been complicated by the fact that aquatic nutrient dynamics are often site-specific, meaning that similar dredging activities can have different chemical effects in different environments [Tramontano & Bohlen 1984]. Of those done in freshwater environments, most have been within the context of dredging as a remediation tactic for hyper-eutrophic lakes, the reasoning being that the removal of nutrient-rich sediments reduces the internal nutrient loading into the lake across the SWI [Liu 2015, Kiani 2020, Zhong 2021]. These studies have shown that dredging is, indeed, usually effective at reducing internal nutrient loading in the short term, though the fate of the removed sediment is rarely followed.

## 1.2 Site Description

The Milwaukee River estuary[1] lies on the western shore of Lake Michigan and consists of the confluence of three rivers in the vicinity of downtown Milwaukee, Wisconsin, USA (Figure 1). The largest (both in terms of drainage area and discharge rate) is the Milwaukee River, whose 1844 $km^2$ (712 $mi^2$) watershed consists not only of urban Milwaukee and its northern suburbs but large stretches of agricultural and forested land as well, stretching across six counties in southeastern Wisconsin [WDNR]. Near its mouth, the Milwaukee River is joined first by the

[1] This study will use the term "estuary" to refer to the Milwaukee River mouth environment to maintain consistency with the terminology used by the USEPA while acknowledging that this environment does not satisfy the strictest definition of the word.

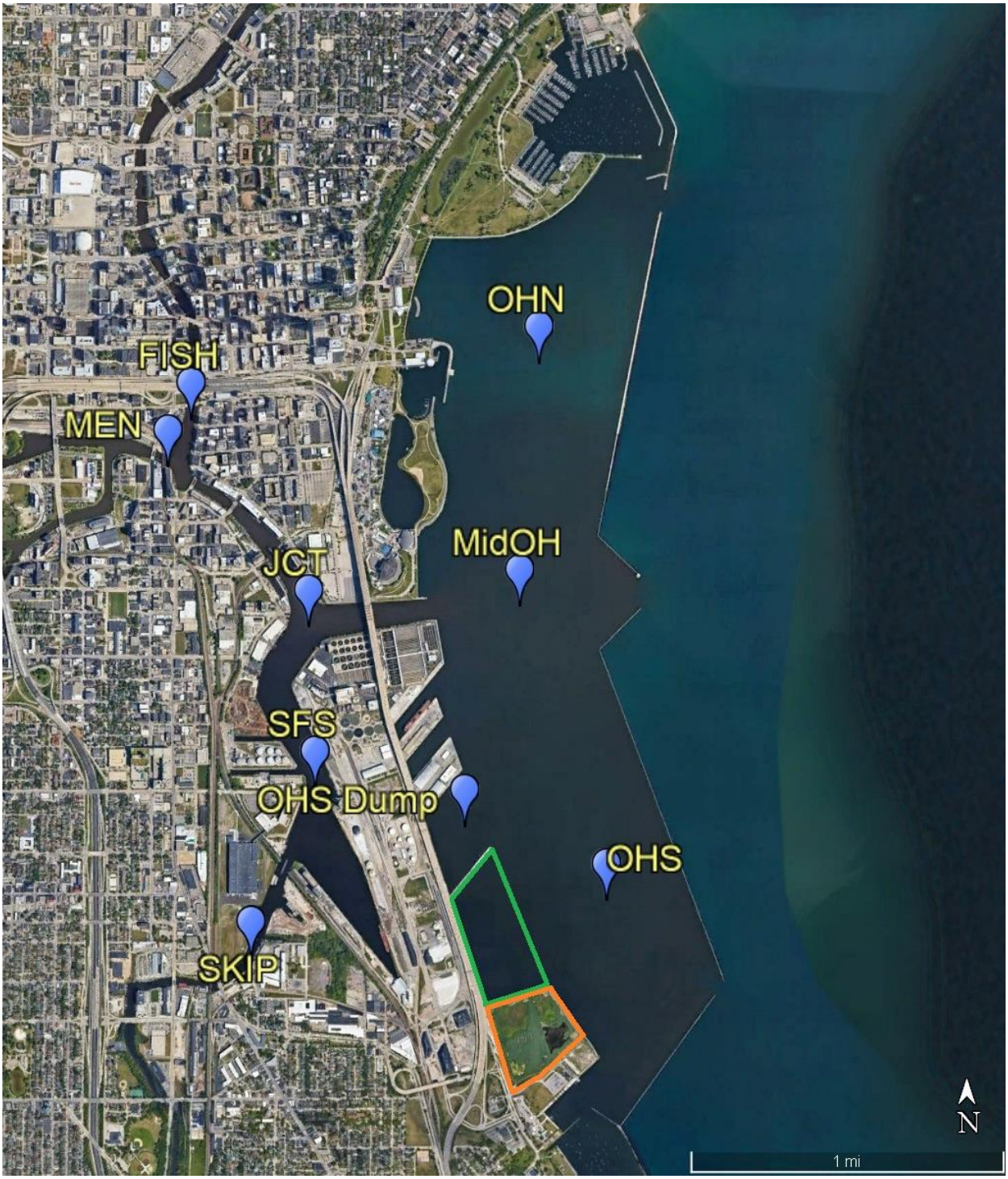


Figure 1: A map of the Milwaukee River estuary with sampling stations. The nearshore stations are not shown. In green: the proposed location for the new DMMF. In orange: the location of the existing DMDF.

Menomonee River, whose 352 $km^2$ (136 $mi^2$) watershed consists mostly of the industrial Menomonee River Valley but also extends well into the western suburbs. The combined flow of these two rivers is then joined by the Kinnickinnic River about 1 km downstream. The smallest and shallowest of the three, the Kinnickinnic River's 85 $km^2$ (33 $mi^2$) basin is almost entirely suburban. The Kinnickinnic River also houses part of Milwaukee's inner harbor area, where the river widens to accommodate freighters.

Before reaching Lake Michigan proper, the combined flow of the three rivers passes through Milwaukee's semi-enclosed outer harbor. Owing to the breakwater, the outer harbor is subject to wind-driven mixing but not to currents on the western shore of the lake. The harbor is also shallow relative to the surrounding nearshore areas. The average depth is about 7-8 m, though it is deeper in the navigation channel that runs straight across the outer harbor from the river mouth to the main gap. This channel and portions of the inner harbor are regularly dredged to allow freighters access to the inner harbor. Historically, the outer harbor is susceptible to seasonal algal blooms owing to the combination of riverine nutrient input and relatively calm, shallow, warm water. These blooms typically occur in late spring and early summer.

Exchange of water between the outer harbor and Lake Michigan occurs at the three gaps in the breakwater, though the bulk of this exchange occurs at the main gap located due east of the river mouth at the end of the navigation channel. Radiochemical tracing has determined that the average residence time of water in the outer harbor is approximately 3.1 days [Montenero 2017]. Generally, the plume of river discharge is largest outside the main gap of the outer harbor, resulting in a difference in water chemistry from that of Lake Michigan proper that is typically measurable up to approximately 1.5-2.5 km (1-1.5 mi) offshore of the gap. This is comparable to

previous studies on nearshore nutrient dynamics immediate to estuaries on the other Laurentian Great Lakes [Howell 2012, Makarewicz 2012a, Makarewicz 2012b].

## 1.3 Dredging the Area of Concern

The Milwaukee River estuary is listed by the United States Environmental Protection Agency as one of 31 Great Lakes areas of concern (AOC) within US-controlled waters, identifying it as a site in particular need of remediation to ensure its continued value to the local population. Of the site's eleven outstanding beneficial use impairments (BUIs), seven of them are directly or indirectly caused or exacerbated by contaminated sediments [WDNR 2021]. The primary contaminants identified in the sediments are polychlorinated biphenyls (PCBs), polycyclic aromatic hydrocarbons (PAHs), non-aqueous phase liquids (NAPLs), and heavy metals [USEPA 2023]. Most recently, poly- or perfluorinated alkyl substances (PFAS) have been identified in the sediments as well [WEC 2020]. Various remedial actions have been taken in the past to address the estuary's multiple BUIs including dredging to remove sediments contaminated with legacy pollutants [USEPA 2023]. At the time of writing, plans have been set in motion for a new, massive AOC-wide dredging project promising the removal of approximately 1.4 million cubic yards of sediment via mechanical and hydraulic dredging [MMSD, WDNR 2021].

Mechanical dredging involves the excavation of sediments, usually via an excavator mounted on a barge. This is suitable for small-scale dredging projects but tends to be slow. Additionally, mechanical dredging often creates large "dredge plumes"—clouds of particulate material suspended as the excavator disturbs the sediment. These dredge plumes are a concern due to the possibility of re-suspending legacy contaminants. Thus, to speed up the process and reduce the effects of dredge plumes, most of the dredging to be done in the Milwaukee estuary

AOC will by hydraulic dredging, in which sediments are loosened by a cutterhead or augur and "vacuumed" up along with water to create a slurry that is then transported via pipeline [Zappi & Hayes 1991]. Schematics of both mechanical and hydraulic dredging are shown in Figure 2. Hydraulic dredging is attractive due to its speed relative to mechanical dredging as well as its tendency to create far smaller dredge plumes. Sediment transport by pipeline also gives hydraulic dredging the ability to move dredged material directly from the removal site to the disposal site over long distances, if necessary. In correspondence with dredging engineers, it is estimated that the average time the slurry will spend in the transport pipeline given the distances between the dredging locations and the disposal site is around 4-5 hours. During this time, the slurry could potentially be the site of a variety of biogeochemical processes that change the chemical character of the removed sediments before they reach the disposal site.

The dredged material will be disposed of at a new Dredged Material Management Facility (DMMF), located on the south shore of the outer harbor directly adjacent to the existing Dredged Material Disposal Facility (DMDF) that contains material from the regular navigational dredging of the harbor [MMSD]. Both facilities are indicated in Figure 1. These are Confined Disposal Facilities (CDFs) designed to prevent direct leaching of contaminants from disposed sediments into surrounding waters through the construction of impermeable barriers. In this case, the proposed barrier consists of a double-walled sheet pile cofferdam filled with granular material and containing a bulk barrier that will be impermeable to water [USACE & MMSD 2023]. This design incorporates additional precautions against direct contaminant leaching than have historically been used in CDFs on the Great Lakes [Miller 1998, Reis 2007, USACE & USEPA 2003]. As the DMMF is filled and the dredged material settles to the bottom, the overlying water (effluent) is removed. Historically, most CDFs on the Great Lakes have

discharged effluent directly into the surrounding waters due to the assumption that target contaminant concentration in CDF effluent is typically acceptably low [Miller 1998, USACE & USEPA 2003]. This has been demonstrated to be true of the types of contaminants whose major pathway of escape from CDFs is via suspended solids in the effluent [See USACE & USEPA 2003 for a list of citations] but may not be applicable to dissolved nutrients. At the time of writing, treatment of effluent is included in construction plans for the Milwaukee DMMF, though the nature of this treatment, and thus its efficacy in addressing nutrient as well as contaminant discharge, is unknown [WEC 2020].

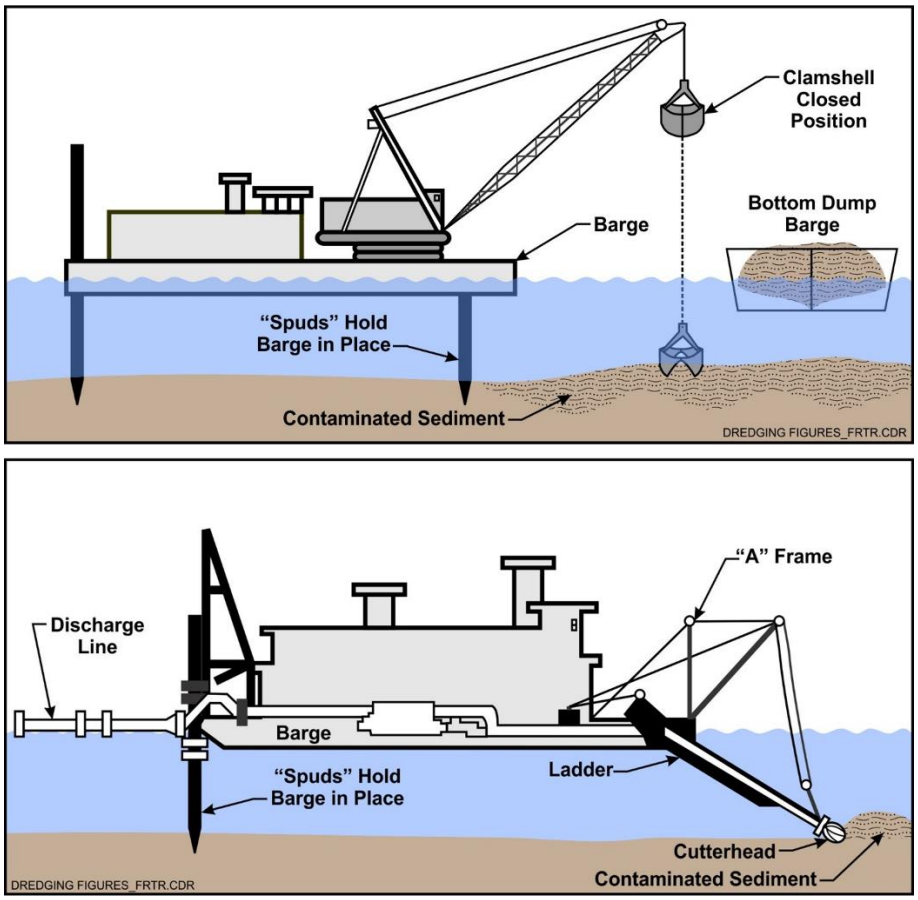


Figure 2: (Top) Schematic of mechanical dredging. (Bottom) Schematic of hydraulic dredging. Here, "Discharge Line" refers to the pipeline that transports contaminated slurry to a disposal site. The pipeline may float on the surface, as shown, or it may be submerged. Reproduced from the Federal Remediation Technologies Roundtable at https://frtr.gov/matrix/Environmental-Dredging/

## 1.4 Dredging-Induced Algal Blooms

Previously, this lab has studied nutrient dynamics surrounding a dredging project on a small, inland lake in southeastern Wisconsin (unpublished). This dredging was much smaller in scale, being for recreational navigation rather than remediation, and only involved the removal of approximately one hundred cubic yards of largely loose, sandy sediment in total. This dredged material was dewatered in large, semi-permeable dewatering bags and the effluent was allowed to run directly back into the lake, as is standard procedure for small-scale dredging of this type. However, the effluent was nutrient-enriched and flowed into a shallow, sheltered embayment in the lake, which triggered a late-season blue-green algal bloom within just a few days of effluent discharge. This bloom was confirmed to include *Microcystis* Cyanobacteria by microscopy, and the water in the embayment was found to have a total microcystins concentration more than 10x the federal limit for recreational waters [USEPA 2019].

It is thought that the toxic Cyanobacterial bloom in this small lake may have been caused specifically by the high total ammoniacal nitrogen (TAN) content of the dredged material. At any given point in time, much of the algal population in Milwaukee's outer harbor, similar to the small lake described above, is comprised not of Cyanobacteria but of diatoms and dinoflagellates which tend to experience increased growth in high nitrate conditions but can sometimes exhibit inhibited growth in high TAN conditions [Blomqvist 1994, Lomas & Glibert 1999a, 1999b, Donald 2011, Glibert 2016]. However, Cyanobacteria behave differently, instead exhibiting increased growth in high TAN conditions due to their preferential usage of ammonium over nitrate [Blomqvist 1994, Donald 2011, Boyett 2013]. This can give Cyanobacteria a competitive advantage in ammonium-enriched waters over diatoms and dinoflagellates. If the total N:P ratio is also high, non-nitrogen fixing Cyanobacteria, such as *Microcystis*, gain even more of a growth

advantage over other alga, which can lead to the formation of toxic algal blooms [Donald 2011, Huisman 2018]. These potential nutrient-driven growth advantages, combined with the dredging of ammonium-rich sediments from the Milwaukee estuary AOC, the knowledge that Milwaukee's outer harbor is going to be the receiving body of the dredged material effluent, and the fact that the outer harbor is already susceptible to seasonal algal blooms, makes the risk of accidently triggering unseasonable algal blooms (potentially toxic algal blooms) in the outer harbor via the introduction of ammonium-rich effluent high enough to warrant an investigation. Unseasonable algal blooms may further impede the beneficial use of the outer harbor, the immediate nearshore areas, and their shorelines for its many shareholders, including civilian (recreational boaters/fishers, beachgoers), business (Milwaukee and South Shore Yacht Clubs, Discovery World, cruise liners), and municipal (Milwaukee Waterworks) interest groups.

## 1.5 Study Objectives

The specific objectives of this study were to examine the nutrient character of sediment porewaters in the Milwaukee river estuary AOC and their dynamics following a simulated disturbance event (including initial mixing, transport, initial dewatering, and continued mixing due to further deliveries to the CDF) that was designed to assess the risk of further nutrient enrichment of the outer harbor and nearshore Lake Michigan. In establishing these underlying chemical data, the groundwork is laid for future work to examine the biological and ecological ramifications, that is, to investigate what risk exists of unintentionally triggering algal blooms in the harbor as a side effect of the removal of legacy contaminated sediments.

# 2 METHODS

## 2.1 Field Sampling

Field samples were collected during four sampling expeditions over the course of approximately one year from the summer of 2022 to that of 2023 on board UWM's research vessel, R/V Neeskay. A map of sampling stations is shown in Figure 1. These stations correspond to different environments within the Milwaukee estuary. A description of each sampling station and its significance to this study can be found in Table 1. In selection of these stations, there was an emphasis in sampling from important locations along the river-lake chemical gradient that characterizes this estuary. The first eight stations (FISH through OHS Dump) are all locations that will eventually be dredged as part of the AOC sediment remediation project, and as such are the primary focus of this study. The last two stations (collectively called the "nearshore" stations) are endpoints of the estuarine chemical gradient and feature the least chemical influence from the Milwaukee rivers relative to the other stations. The nearshore stations are not locations that will be dredged. One of the sampling expeditions was in midwinter (18 January) when all sampling locations, including the nearshore stations, were experiencing complete mixing of the water columns. During the other three expeditions, some degree of water column stratification is present at most or all of the stations, except the "upriver" (relative to JCT) FISH, MEN, SKIP, and SFS stations.

Table 1: Sampling station descriptions

| Station ID | Description |
|---|---|
| FISH | Up the Milwaukee River as far as the St. Paul Ave. bridge; the chemical environment of the Milwaukee River outflow. |
| MEN | Up the Menomonee River as far as the first railroad bridge (approximately one ship's length past the river mouth); the environment of solely the Menomonee River |
| SKIP | Up the Kinnickinnic River as far as the Skipper Bud's Marina on S Marina Dr., just before the river gets too shallow to continue; the environment of the Kinnickinnic River. |
| SFS | Located just off the east end of the UWM School of Freshwater Sciences building at 600 E Greenfield Ave.; the environment of the southern inner harbor. |
| JCT | The confluence (or junction) of the three rivers. |
| MidOH | The middle of the outer harbor, in the navigation channel. |
| OHN | The northern section of the outer harbor, approximately equidistant from the navigation channel and the north gap in the breakwater. |
| OHS | The southern section of the outer harbor, closer to the south gap in the breakwater than the navigation channel. |
| OHS Dump | Closer to shore than OHS and partially secluded by piers. This is the approximate location of the northern edge of the proposed DMMF, and is the environment that effluent or leachate form the facility discharged directly into the harbor would enter. |
| LW 50 | Nearly 11 km northeast of the main gap in the harbor breakwater at a depth of about 50 m; an environment with only slight chemical influences from the Milwaukee area. |
| Fox Pt | Just over 25 km northeast of the main gap in the harbor breakwater at a depth of about 100 m; the environment of Lake Michigan relatively free of chemical influences from the Milwaukee area. |

All stations were sampled for surface sediment via a PONAR grab, as well as surface and near-bottom water (1 m off the bottom, or B-1) by bucket and Niskin bottle, respectively. Not every station was visited on every expedition. Sediment samples were unloaded from the PONAR into a rinsed fiberglass tray. When subsampling from the PONAR grab, efforts were made to collect as little debris and as few mussels (*Dreissena*) and other benthic organisms as possible. To this end modified 140 cc syringes with the ends cut off were used to suction "cores" from the bulk sediment sample, which were then transferred to completely fill polycarbonate

bottles for eventual centrifugation. This also exposed the subsamples to minimal contact with air during handling. Separate subsamples were collected in Whirl-Pak® bags and sealed immediately, also to minimize atmospheric contact, for use in sediment leaching experiments (section 2.4). Because a PONAR grab does not reliably preserve the stratification of surface sediments, subsamples were shaken in the receiving containers to homogenize them in order to acquire an "average" sample of the surface layers of sediment.

Multi-parameter sondes (SeaBird or OTT Hydromet) were also used at all sampling locations to obtain a number of measurements, though the only parameters that are utilized in this report are dissolved oxygen, temperature, and conductivity with the latter two used primarily to demonstrate bi-lateral stratification at estuarine stations.

## 2.2 Chemical Analyses

Water and sediment porewater samples were analyzed for Total Ammoniacal Nitrogen (TAN), nitrate ($NO_3^-$), nitrite ($NO_2^-$), Dissolved Organic Nitrogen (DON), Soluble Reactive Phosphorus (SRP), Filterable Phosphorus (FP), Dissolved Inorganic Carbon (DIC), and Dissolved Organic Carbon (DOC) by a combination of methods, described below. Total Ammoniacal Nitrogen (TAN) refers to the combination of ammonium ($NH_4^+$) and ammonia ($NH_3$), the two most reduced forms of nitrogen that readily interconvert in neutral pH conditions. Dissolved Organic Nitrogen (DON) refers to the organic fraction of Total Dissolved Nitrogen (TDN, defined as all nitrogen that passes through a 0.2 μm filter), and is calculated as the difference between TDN and Dissolved Inorganic Nitrogen (DIN, determined as the sum of TAN, nitrate, and nitrite). Soluble Reactive Phosphorus (SRP, also called orthophosphate) refers to the forms of dissolved phosphorus that are readily bioavailable to algae and other

microorganisms. Filterable Phosphorus (FP) refers to the combination of SRP and all other forms of dissolved phosphorus, defined as those forms that will pass through a 0.2 μm membrane. Dissolved Inorganic Carbon (DIC) refers to the sum of carbonate ($CO_3^{2-}$), bicarbonate ($HCO_3^-$), carbonic acid ($H_2CO_3$), and dissolved carbon dioxide ($CO_2$). These four carbon species exist in equilibrium with each other, the dominant form depending on the pH of the solution. Dissolved Organic Carbon (DOC) is the chemically heterogenous organic fraction of Total Dissolved Carbon (TDC), the inorganic fraction being DIC.

Nitrite, SRP, and FP were measured by spectrophotometry. Nitrite was determined at 543 nm by reaction with sulfanilamide, while SRP and FP were determined at 880 nm by reaction with acidified molybdate in the presence of ascorbic acid [Hansen & Koroleff 1999]. Sample concentrations were quantified by referencing absorbances to those of known standard concentrations. Standard ranges were determined such that unknowns were within the total range by visual comparison of color development within the analytical matrices. Multiple standard sets were periodically read alongside sample sets to account for instrumental drift over the course of longer analysis sessions. The path length was either 1, 5, or 10 cm depending on the sample concentrations, with standard ranges changed accordingly. Most phosphorus analyses were performed by Sharon Zsebe, UWM School of Freshwater Sciences.

Dissolved Inorganic Carbon (DIC) was determined by flow-injection conductimetry via pH forced conversion of $CO_2$ to carbonate across a semipermeable Teflon membrane [Hall & Aller 1992]. Samples are injected into a continuous flow of 10 mM hydrochloric acid passing over one side of the Teflon membrane, with 7.5 mM sodium hydroxide passed along the opposite side. In acidic conditions, all DIC ($CO_3^{2-}$, $HCO_3^-$, $H_2CO_3$ and $CO_2$) is transformed into gaseous $CO_2$,

which crosses the semipermeable membrane. In basic conditions on the other side, the $CO_2$ converts to $CO_3^{2-}$, which is then quantified by conductimetry.

Nitrate was determined by a flow-injection spectrophotometric method. Samples were injected onto a cadmium reduction column, where all nitrate was transformed into nitrite that can then be quantified spectrophotometrically with a method analogous to that used for nitrite alone. This method technically determines the sum concentration of nitrate + nitrite, and is annotated as such in all figures to follow, but is usually interpreted as solely nitrate due to nitrate usually being at least an order of magnitude more concentrated than nitrite. Where necessary due to relatively high nitrite or low nitrate concentrations, the true nitrate concentration is determined by the difference between the nitrate + nitrite value determined by flow-injection and the nitrite value determined by spectrophotometry.

Total Dissolved Nitrogen (TDN) and Dissolved Organic Carbon (DOC) were both determined by a Shimadzu TOC-L analyzer. They are initially quantified as Total Nitrogen (TN) and Non-Purgeable organic Carbon (NPOC) by those respective methods as described by Shimadzu. Pre-filtration of the samples through a 0.2 μm membrane limits TN to only TDN, from which DON is calculated as the difference between TDN and DIN. The NPOC results are interpreted as approximately equal to Total Dissolved Carbon (TDC) under the assumption that the total concentration of purgeable, volatile carbon is negligibly low in both water and surface sediment porewater samples, and its loss via sparging is inconsequential[2]. This is further limited to only DOC by the assumption that all DIC is also removed as $CO_2$ during sparging. Both DON and DOC were measured by Tim Wahl, UWM School of Freshwater Sciences.

[2] It is possible that methane ($CH_4$), methyl mercury ($CH_3Hg$), and methyl chloride ($CH_3Cl$) are present in porewater.

### 2.2.1 Determination of TAN

The analytical procedure for Total Ammoniacal Nitrogen (TAN) was complicated due to the complexity of the porewater matrices. Eventually, TAN came to be determined by either spectrophotometry or flow-injection conductimetry depending on concentration, but the process to arrive at this procedure warrants further explanation.

For relatively low concentration samples (< 250 μM), TAN was determined by spectrophotometry at 630 nm by reaction with hypochlorite, phenol, and ferricyanide [Hansen & Koroleff 1999]. Low concentration samples included all water samples and most leaching samples (see section 2.4 below) as well as some porewaters, mostly from the outer harbor or nearshore stations. Relatively high concentration samples (> 250 μM) were analyzed for TAN by flow-injection conductimetry by pH forced conversion of TAN to ammonia across a semipermeable Teflon membrane [Hansen & Koroleff 1999]. This method is analogous to the method used to determine DIC, but with the acidic and basic carriers reversed because gaseous $NH_3$ is predominant in basic conditions. Not only is this flow-injection method faster and easier than the spectrophotometric method, but it resolved an issue with matrix interferences that were sometimes experienced when analyzing porewater samples containing additional redox-active substances (e.g. $H_2S$, $Fe^{2+}$).

Sediment porewater samples were far more complex solutions than lakewater and required additional precautions and sensitivity modifications. However, matrix interference from the plethora of dissolved material in the porewater samples was reduced in most cases by necessary dilution for accurate quantification. The exception was TAN, the analysis of which suffered from a positive matrix interference that caused particularly highly concentrated porewater samples (JCT was the most commonly affected) to read spectrophotometrically much

higher concentrations of TAN than were expected. This discrepancy was not discovered until the flow-injection conductimetric method was first used on the porewater samples from 11 May. After that point all porewater samples were first read by flow-injection. This method was considered more accurate due to the lack of matrix interferences. Those with a TAN content too low to be quantified by that method (< 250 μM) were re-analyzed by spectrophotometry. Positive-error matrix effects were only significant in the highly concentrated samples. By May 2023, though, it was too late to accurately re-read the samples from 25 July, 2022 and 18 January, 2023. It is likely that the reported values for those samples are higher than the actual values, potentially up to about 32% (the high end of the positive error found in the 11 May samples) though likely much lower than this for all but JCT.

The exact cause of the matrix interference is unknown. The original source of most of the analytical methods used in this study [Hansen & Koroleff 1999], cites Zadorojny 1973 as identifying cyanide, thiocyanide, and sulfide as three of 25 possible interferences in seawater that can cause a significant positive error when determining TAN by spectrophotometry. Of those three, sulfide seems to be the most likely candidate, as the anoxic conditions that prevail in sediments below approximately a millimeter of depth may allow for the bio-reduction of sulfate into sulfide (see Appendix A). Additionally, Zadorojny notes that the presence of certain amino acids can cause a positive error in the analysis possibly due to hydrolyzation in the extremely alkaline (pH > 11) analytical matrix. The highest reported error was 103% for L-threonine and L-lysine-HCl, which is not high enough to explain the observed errors (up to 32%) in the porewater analyses by spectrophotometry alone but could still be contributing.

## 2.3 Preparatory Procedures for Porewater

Sediment samples were centrifuged in acid-washed polycarbonate bottles or centrifuge tubes at high speed (~18-20,000 RCF) for 30 minutes to separate out fluids from solid material. The raw porewater was then decanted off and filtered first through GF/F glass fiber membranes (Whatman) then through 0.2 μm PES filters (Pall Supor®) to further separate the dissolved material. Centrifuging this decanted porewater a second time before filtration was tried but did little to ease the filtering process. The resulting 0.2 μm filtered porewater samples were analyzed for all of the same dissolved nutrients as the water samples by the same methods as described in section 2.2.

Alongside porewater chemical analyses, porewater water contents were determined by weighing separate sediment aliquots and drying them in a 60 ℃ oven. After these aliquots achieved a reached a constant weight (determined after successive measurements), the water content by weight was determined by the difference between dry and wet weights.

### 2.3.1 Evolution of Porewater Procedures

The first iteration of the porewater separation procedure involved spinning whole mud samples in 500 mL polycarbonate centrifuge bottles at ~18000 RCF for 45 minutes in a Beckman J2-21 model floor centrifuge. Not only did this successfully separate the porewater from the solid material, but the bottles were large enough to be easily filled on-site directly from the PONAR sample and the volume of porewater obtained from a full bottle of sediment (usually around 150-200 mL) was more than enough for the full range of chemical analyses that are typically done for this study. In September 2022, however, this centrifuge irreparably broke down. Unfortunately, this coincided with a sediment sampling from early September, which in the time it took to develop an alternative separation procedure had aged too long to be accurately

quantified for the most labile nutrients, hence why those samples make no appearance in this report.

Eventually, an alternative procedure on a different centrifuge, an Eppendorf 5810R, was developed. This centrifuge was capable of the same RCF as the Beckman J2-21 but could only hold up to 80 mL tubes. This resulted in a far smaller porewater return for each sample (approximately 25-35 mL, depending on the water content) and due to the difficulty of acquiring more centrifuge tubes (a holdover from COVID-era supply chain disruptions), reading duplicate tubes for each sediment sample would have added days of work for each porewater analysis. Instead, it was decided that some analyses would simply need to be sacrificed, namely FP and DON/DOC. Their exclusion saved nearly 20 mL of each sample. This procedure would be used for the 18 January and 11 May sample sets, for both porewater and leaching experiments. By the time of the 20 June sampling, a replacement Beckman J2-21 centrifuge had been acquired, and the original separation procedure was used again.

The post-centrifugation filtration procedure was also subject to some minor adjustments over time. In testing, it was discovered that simply pressure-filtering separated porewater fresh from the centrifuge through a 0.2 micron syringe filter was not adequate, as the filters would clog almost immediately. By first passing porewater through a glass fiber filter, this was mitigated. Placing both filters in the same reusable syringe filter cartridge (one on top of the other) resulted in excessive leaking out of the sides of the cartridge, and thus lost sample volume. This became a particular concern after the separation procedure was changed and sample volumes were greatly reduced. The filtration process was eventually streamlined by attaching disposable 0.2 micron PES filter cartridges (Pall) directly to the outlet of a reusable filter cartridge housing a GF/F, which leaked far less and could be quickly replaced, greatly increasing

efficiency. Using this method, approximately 25-40 mL of particle-free porewater could be reliably obtained for every ~70 mL of whole sediment aliquot.

## 2.4 Porewater Leaching Experiments

To ascertain how nutrients leach out of the sediments and how they transform over time following a disturbance, slurries were created with 90 mL sediment aliquots mixed with 810 mL 0.2 μm filtered harbor water (1:10 v/v dilution of whole sediment) and continuously rolled in 1 L polycarbonate bottles. These leaching experiments (or "rolling experiments") have been shown to recreate analogous hydrodynamic conditions to a sediment-water interface under continuously flowing water, such as a river or freshwater estuary [Aguilar & Cuhel 2023], though in this study they are used to approximate the movement of sediment and water through the slurry transport pipeline. A time series of samples was collected from the bottles over a period of approximately 2-4 weeks, with emphasis on an initial sampling immediately after mixing ($t_0$ corresponding to the disturbance of the sediment as it is removed) and a second sampling within four or five hours of mixing ($t_1$ approximately corresponding to the time the sediment slurry will spend travelling through the pipeline). Later time points ($t_2$-$t_3$) during the experiment are designed to approximate the type of long-term, sustained disturbance that the surface sediments may experience within a CDF as new material is gradually deposited. An example time series may be: t+0 days, +0.2 days (5 hours), +2 days (48 hours), +14 days (2 weeks). In the first two experiments (25 July, 2022 and 18 January, 2023) an additional $t_4$ time point at +26-28 days (4 weeks) was sampled[3]. The exact timing of each sampling point varied from experiment to experiment, but approximately

[3] Not all chemical analyses were performed on the $t_4$ samples from the 25 July, 2022 experiment. For SRP and DOC, the last analyses were done at $t_3$ (10 days).

followed the above intervals. At each point, bottles were shaken to mix their contents before sampling. This was done so that each sampling contained an approximately equal sediment-to-water ratio, preserving the original 1:10 sediment-to-water ratio for future samplings. These samples were analyzed for the same nutrients as the initial porewater samples following the same centrifugation and filtration procedure.

Leaching experiments were performed four times following the sampling expeditions on 25 June, 2022, 18 January, 2023, and 11 May, 2023. Two experiments were performed on the 11 May samples. During the 25 June experiment the bottles were periodically opened to refresh the air inside, reducing the risk of oxygen depletion. This was repeated for the 18 January experiment, but chemical evidence suggested that the water in some samples possibly became anoxic at some point during the experiment due to the bottles not being opened frequently enough. To verify this, the 11 May experiment consisted of both an "oxic" set, wherein the bottles were opened frequently to ensure adequate oxygen supply, and an "anoxic"[4] set consisting of sealed syringes instead of bottles opened only when sampling to ensure that the water would eventually turn anoxic similar to what was suspected to have happened in the 18 January samples. These syringes were placed on a gyro-rotation table under the assumption that this would approximate the continuous motion of water over the surface of the sediment in the same way as the rolling bottles, but this was not the case. The gyro table did not move the contents of the syringe to the same extent as the rolling bottles, greatly reducing the rate of nutrient exchange into the water (as previously demonstrated by Aguilar & Cuhel, 2023).

[4] Dissolved oxygen was never measured itself. The labels "oxic" and "anoxic" are used to differentiate between the two leaching experiments done using the 11 May sediment samples based on observed chemical dynamics.

Despite the slower rate of nutrient leaching, the observed chemical dynamics imply that anoxic conditions were likely still achieved in the syringes, allowing some degree of verification of the results from the 18 January experiment.

It was often the case in the leaching experiments that nutrients were released into the receiving water in far higher concentrations than would be predicted by the dilution of the initial porewater contents alone. This is demonstrated in Figures 14, 17, 21, 25, 26 and 35. The "Expected Dilution" values in these figures are calculated from the initial porewater concentrations diluted 1:10 after adjusting for the water content of the sediment samples (Shown in Figure 4). The specific equation used to calculate expected dilutions was:

$$ED = (DF_S * WC * C_P) + (DF_W * C_W)$$

Where $ED$ is the expected dilution, $DF_S$ is the dilution factor of sediment aliquots (0.1 in all experiments), $WC$ is the water content of the whole sediment expressed as a fraction, $C_P$ is the porewater concentration of the analyte of interest, $DF_W$ is the dilution factor of the receiving water (0.9 in all experiments), and $C_W$ is the initial concentration of that analyte already present in the receiving water. This calculation yields a theoretical maximum concentration in the receiving water wherein all dissolved analyte content of the porewater is leached into the receiving water in the absence of any biogeochemical effects.

A schematic for the total workflow following each sediment sampling is shown in Figure 3. Depending on which centrifuge was used, sediment aliquots into centrifuge tubes for porewater separation was not always necessary.

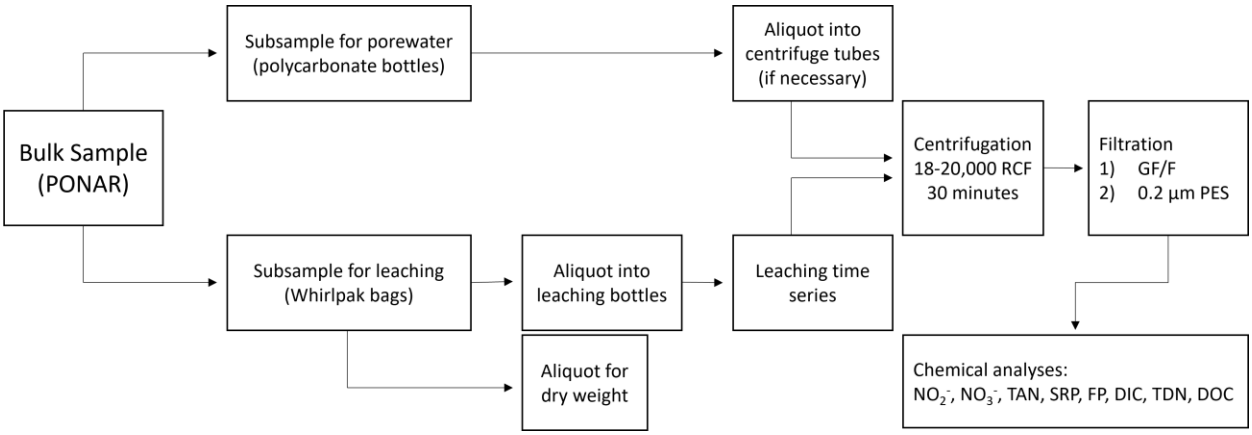


Figure 3: Generalized schematic of the analytical workflow for this project.

# 3 RESULTS

## 3.1 Physical Character of Surface Sediments

Sediment samples from throughout the estuary were comprised mostly of fine silt rich in organic material. MidOH and JCT were generally less fine, which may be due to high commercial boat traffic over these stations stirring up the surface sediments. Surface sediment water contents at the river and harbor stations were between 35-75% w/w (Figure 4). Of the seven stations that were sampled multiple times, only OHN displayed a range of less than 5% among sampling dates. The other six stations experienced more variability in water content over time, often increasing compared to the previous date(s). Due to the frequent, but seasonal, passage of large freighters in the deeper portions of the harbor and smaller ships in the shallower portions, surface sediments throughout the estuary are often disturbed. This likely affects not just the water content, but also the chemical character of surface sediments observed between locations especially during April-November.

The range in water contents observed in these surface sediments is significant to the mechanics of dredging itself. As described above, hydraulic dredging involves the transport of

dredged material to a CDF by pipeline. This necessitates mixing the solid material with water to form a slurry, depending on the water content of the sediment—the lower the water content, the more water needs to be added to achieve a transportable slurry. An approximate water content of 40-60% in the slurry seems to be ideal, based on correspondence with dredging engineers. The surface sediments in the AOC already have this much water in them, so when dredging only the surface, little water may need to be added to create a transportable slurry. Below the surface, however, the water content of sediments is expected to decrease to as low as ~20% w/w by about 3 meters in depth [Menounos 1997] and more water will need to be added to the pipeline. This will affect chemical fluxes within the pipeline, and is an idea that will be revisited in discussion of observed nutrient dynamics.

Sediment samples from some stations had a strong odor to them, reminiscent of sewage. In particular, JCT often had a strong odor that lingered in the extracted porewater, as did the other river samples and OHS Dump to lesser extents. The odor of these porewaters tended to fade to imperceptibility in most samples after approximately two weeks in storage, except for JCT. Porewater extracted from these samples tended to develop a color after filtering that ranged from faint yellow to a rusty orange. The nearshore samples, OHN, and OHS porewater samples never had any perceptible odor or color. It is hypothesized that the color may be due to the formation of iron colloids (perhaps with adsorbed phosphate or sulfate), as the color could be effectively removed by re-filtering the sample. Further evidence supporting the iron-phosphate colloid hypothesis was found when porewater that had been re-filtered to remove the color had a lower SRP content than their predecessors. Phosphorus analyses in the initial porewater samples, conducted immediately after centrifugation, were unaffected. The odor may be due to anaerobic sulfate respiration generating hydrogen sulfide.

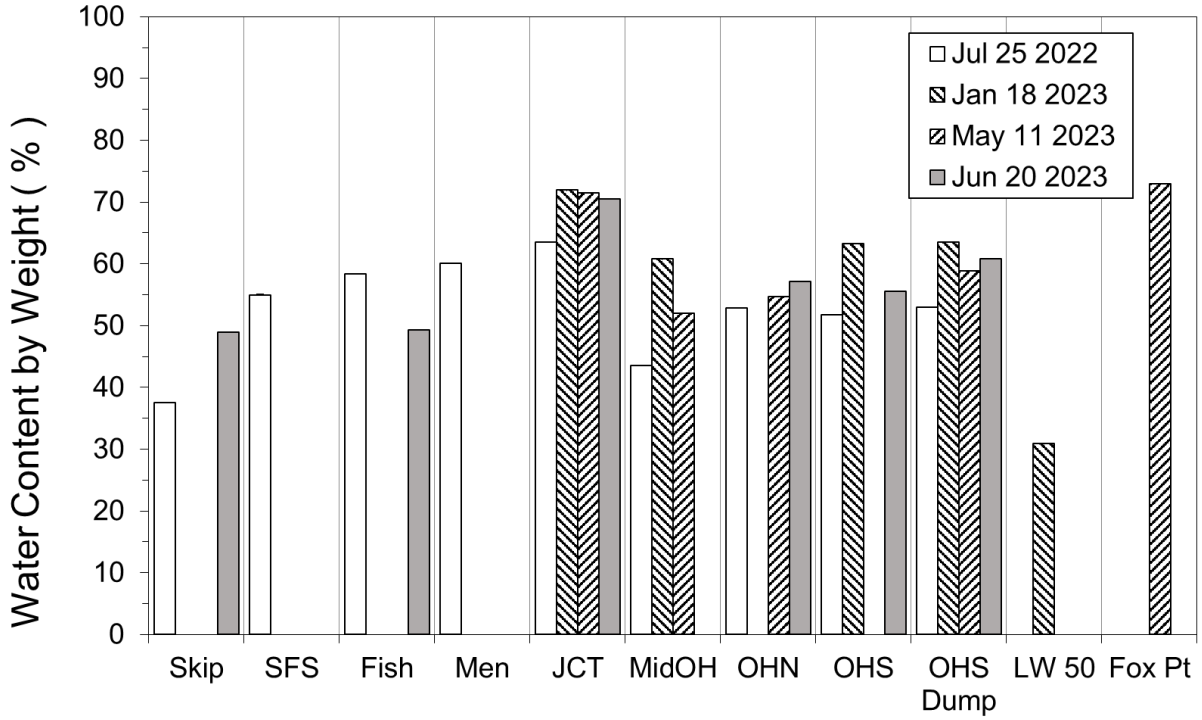


Figure 4: Water contents of whole sediment samples determined by drying to constant weight.

## 3.2 Chemical Dynamics of Sediment Nutrients

Nutrient contents of surface sediments porewaters exhibited large variation among location and sampling dates, particularly in the rivers and MidOH. The OHN and OHS stations were not only relatively similar to each other on all sampling dates but showed far less temporal variability than the other stations. OHS Dump was chemically very different from the other outer harbor stations, often more closely resembling the river stations. The nearshore stations were generally less nutrient enriched than the other stations, with the exception of nitrate at LW50.

Also of note is the constant, approximately neutral pH that was maintained throughout the 25 July, 2022, experiment (pH was not measured in future experiments). Many of the

biogeochemical processes to be discussed affect and/or are affected by the acidity of the environment.

### 3.2.1 Nitrogen in Porewater

Most dissolved inorganic nitrogen in surface porewater tended to be in the form of total ammoniacal nitrogen (TAN) rather than nitrate or nitrite, often by a difference of at least one order of magnitude (Figure 5). Many stations had porewater TAN concentrations over 1000 μM for at least one sampling date—JCT had over 1000 μM TAN on three of the four dates. Stations OHN and OHS were much less enriched than both the river stations and the other harbor stations and the nearshore stations were quite low by comparison.

Crucially, porewater at nearly every station was always far more enriched in TAN than the overlying water columns. When disturbed, this porewater can enrich the receiving waters. There is a notable exception found at MidOH on 20 June, which saw a much higher concentration of TAN near the bottom than the surface—0.4 μM vs. 8.3 μM at the surface and bottom, respectively—approximately an 20x increase from the surface concentration. This sample is revisited in more detail in section 4.1.

Nitrate and nitrite combined (Figure 6) were usually between 1-20 μM excluding LW50, with nitrite alone (Figure 7) constituting only a small quantity (< 1 μM) with exceptions at JCT, MidOH, and OHS Dump where nitrite concentration was similar to nitrate. LW50 was the only station that was ever more enriched with nitrate than TAN (70 μM vs. 1 μM, respectively), a situation that is not replicated in the Fox Pt sample, the only other nearshore station. Unlike TAN, both nitrate + nitrite and nitrite alone were present in porewaters at concentrations at or below what was found in the overlying water columns with a handful of exceptions (LW 50 on 18 January for nitrate, MidOH and OHS Dump on 25 July for nitrite). Both were slightly

elevated in surface waters versus B-1 waters at some stations, which was likely caused by atmospheric deposition. Porewater was also highly enriched in organic nitrogen at all stations, more similar to TAN than the oxidized forms, again with OHN and OHS being both less enriched and less temporally variable than the other stations (Figure 8). The full species distribution of dissolved nitrogen in surface sediments is shown in Figure 9.

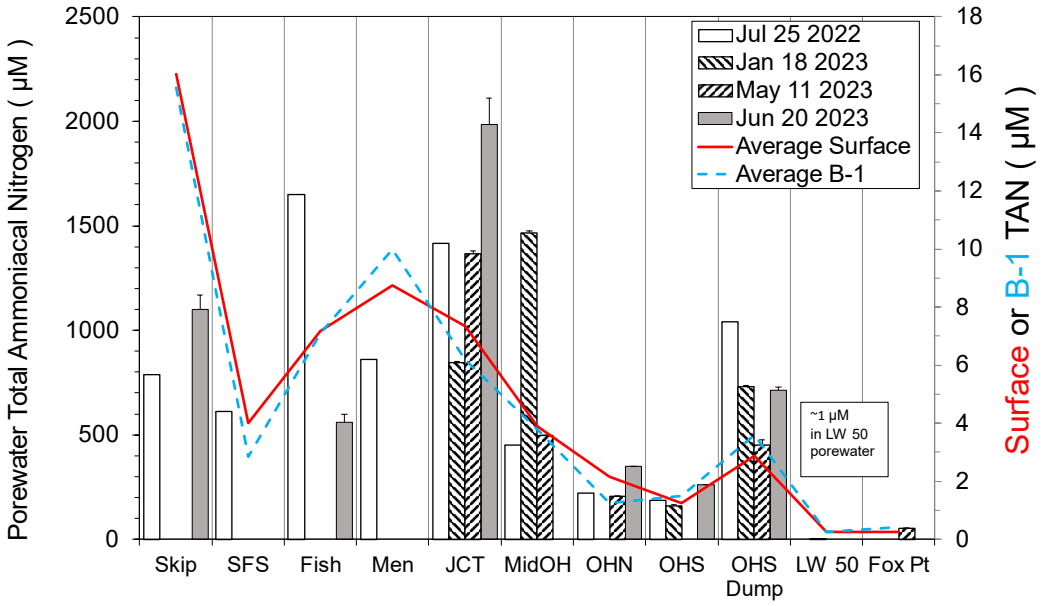


Figure 5: Total ammoniacal nitrogen contents of surface sediment porewaters and their respective water column averages. Most sediments were over 100x higher in TAN than their corresponding waters except LW 50 and Fox Pt. LW50 had a TAN content of about 1 µM—too low to appear on the graph.

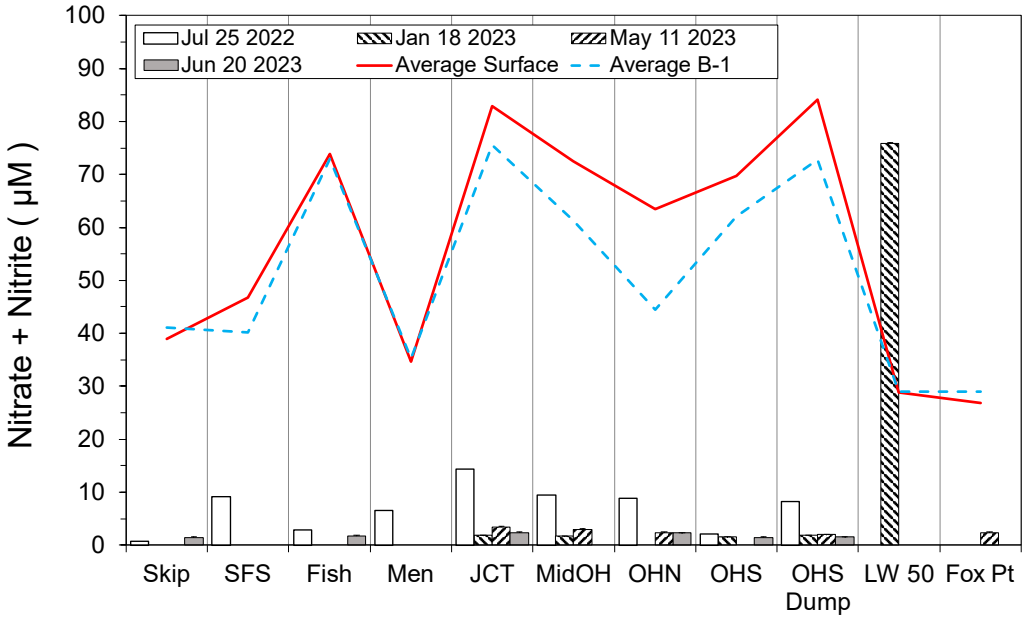


Figure 6: Nitrate + Nitrite contents of surface sediment porewaters and their respective water column averages. Except for LW 50, all porewaters had less nitrate + nitrate than their water columns. Nitrate + nitrite was often enriched slightly in the surface waters compared to B-1. This is most likely due to infiltration from the atmosphere.

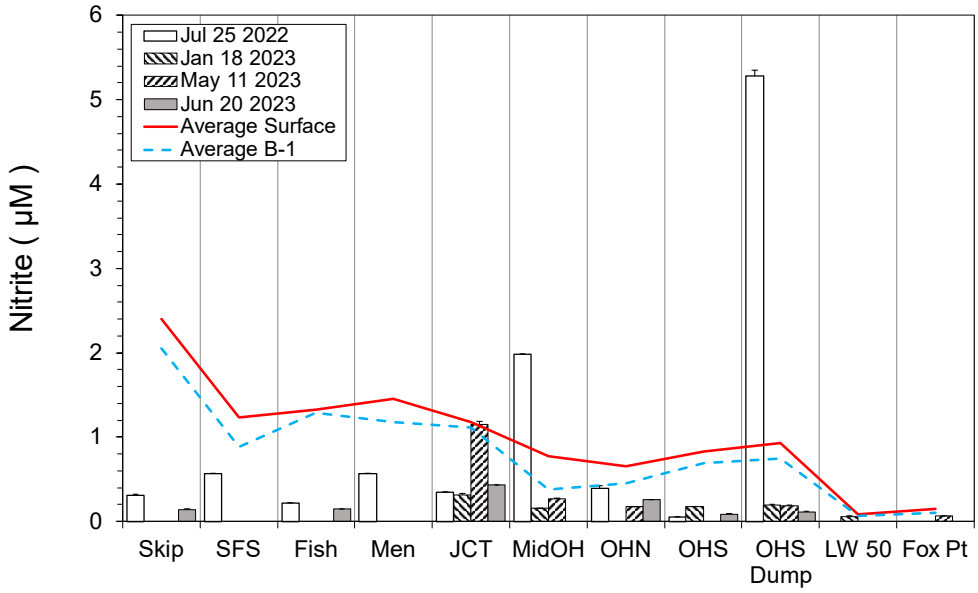


Figure 7: Nitrite contents of surface sediment porewaters. Porewaters were mostly at or below water column concentrations except for MidOH and OHS Dump on 25 July, 2022. Nitrite was slightly elevated in surface waters over B-1 waters. Like with nitrate, this is likely due to atmospheric influence.

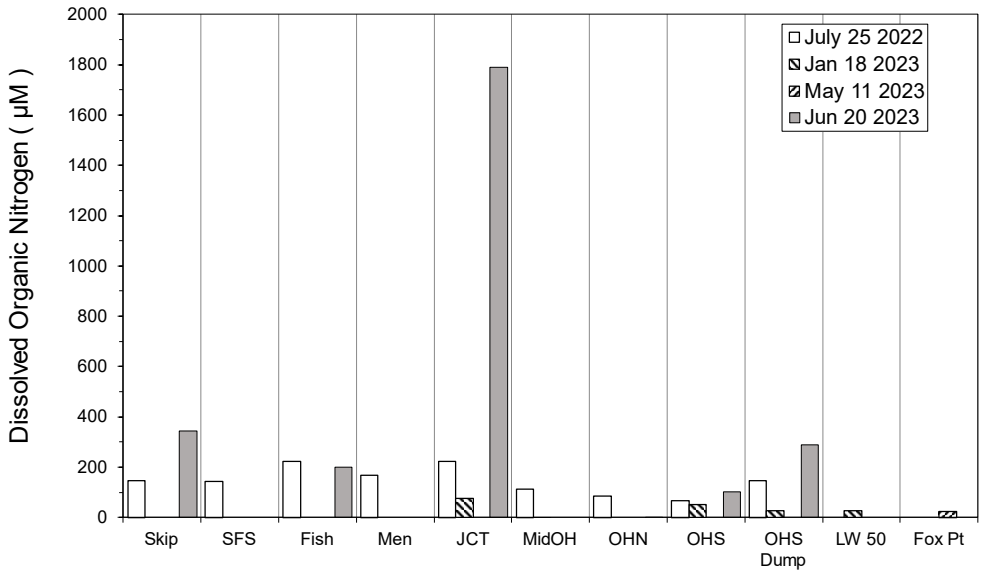


Figure 8: DON contents of surface sediment porewaters. Note that two samples (18 Jan MidOH and 20 Jun OHN) are negative. This is likely due to TDN being undercounted, as can happen if too much time passes after the DIN is measured and gaseous ammonia is given time to escape from solution. It is likely that DON is simply very low. Only Fox Pt DON was calculated from the 11 May sample set.

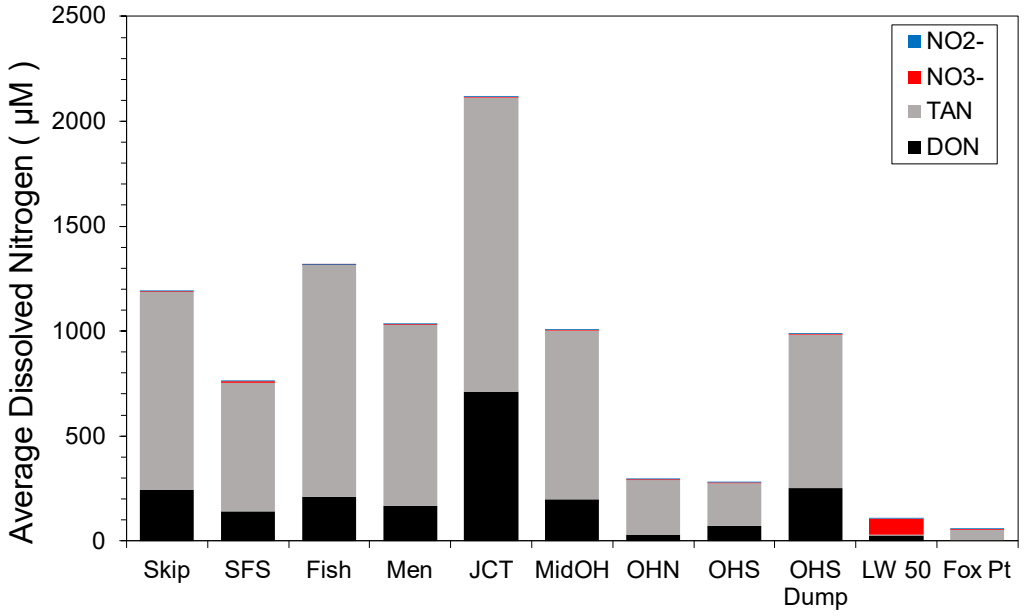


Figure 9: Average total dissolved nitrogen (TDN) contents of surface sediment porewaters across all sampling expeditions.

### 3.2.2 Nitrogen Disturbance Dynamics

The dynamics of dissolved nitrogen following a disturbance in the sediment varied depending on the speciation. In the 25 July and 11 May sediment leaching experiments, TAN tended to reach a maximum just a few hours after the initial mixing ($t_1$) then rapidly decreased to near zero (Figures 10 & 11, top). These TAN enrichments at $t_1$ reached concentrations far higher than what would be expected based on a simple 1:10 v/v dilution of sediment into water, with a leaching return between 4-10x higher than expected (Figure 14). Nitrate rose steadily over time with the river sediments reaching much higher end values after 2-4 weeks than the harbors, but the nearshore Fox Pt sample did not significantly rise at all (Figures 10 & 11, middle). There was no initial, rapid increase in nitrate concentration following mixing in any sample. Nitrite concentrations peaked around $t_1$ or $t_2$, with the true maxima likely in between, then decreased more gradually over time often remaining elevated two weeks later ($t_3$) (Figures 10 & 11, bottom).

In the 18 January experiment, following the enrichment in TAN after the initial mixing and subsequent drop, concentrations began to gradually rise again in the JCT and MidOH samples throughout the remainder of the experiment, possibly as a result of organic decomposition or denitrification in anoxic conditions (Figure 12, top). This increase in TAN was accompanied by a simultaneous decrease in nitrate in the same samples (Figure 12, middle). The TAN increase was recreated in the anoxic syringe experiment with the 11 May sediment samples, but only in JCT which rose over 150 μM over the initial concentration—similar to the 18 January bottles but miniscule compared to the initial TAN enrichment of the oxic experiments (Figure 13, top). The other samples fell over time, but only gradually instead of abruptly like the oxic experiments, and never decreased to low concentrations relative to the initial. This may

indicate the presence of TAN-producing processes slowing the decrease in TAN over time, if not completely reversing it as may be the case in the JCT sample. As for nitrate + nitrite, in the 11 May anoxic syringes it dropped precipitously to about 3 μM in all samples and stayed there through the end of the experiment (Figure 13, middle). Nitrite exhibited the same initial enrichment and subsequent decrease in the syringes as the oxic bottles, but the peak concentration was at most only half as much as in the 18 January in every sample, likely due mostly to the slower release of nutrients due to the rolling conditions in the syringes (Figure 13, bottom).

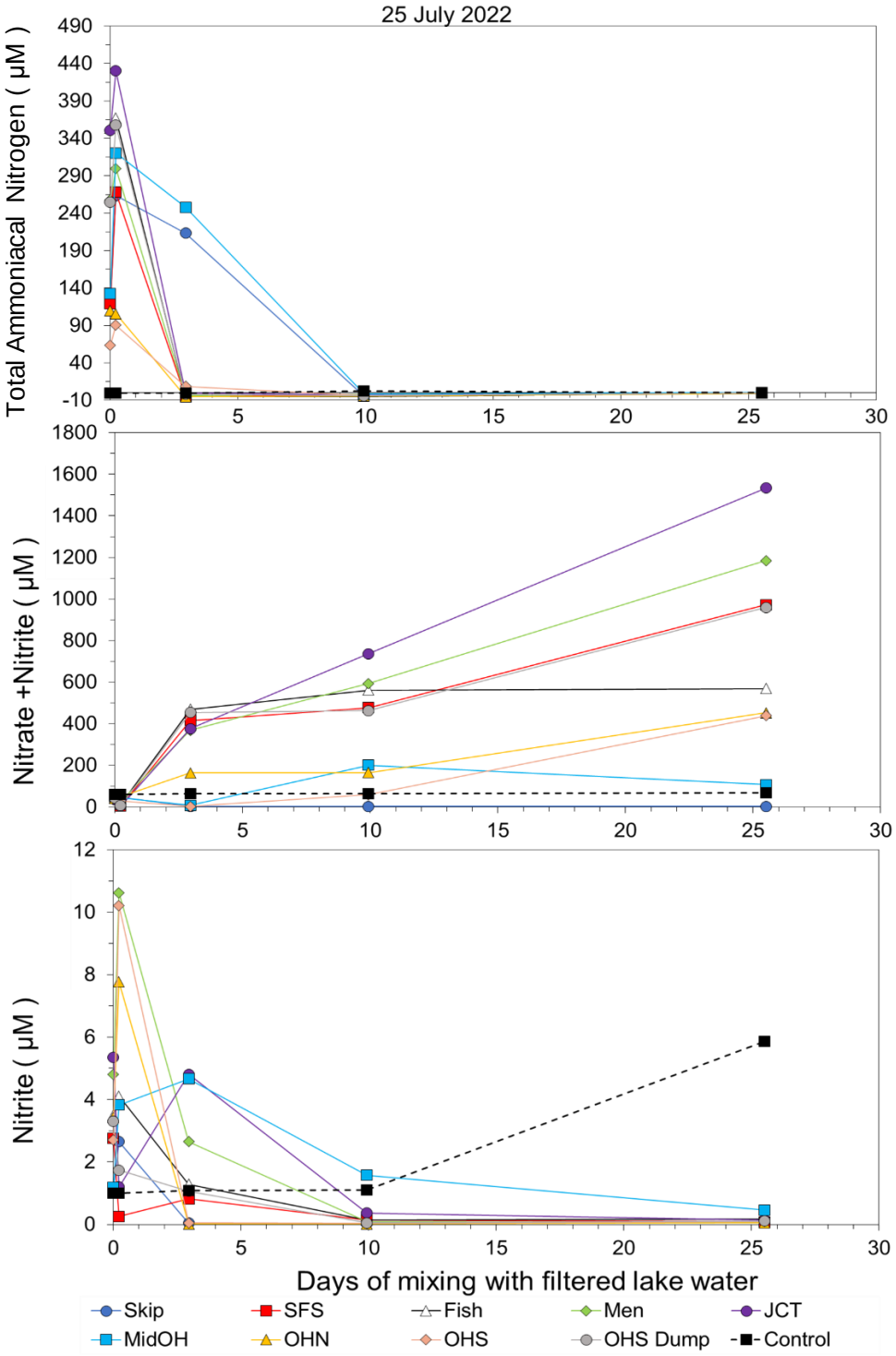


Figure 10: Dissolved inorganic nitrogen dynamics from the June 15, 2023 porewater leaching experiment. In all samples, TAN concentrations dropped to very low levels by 10 days, some as early as 3 days. This was accompanied by a rise in nitrate + nitrite, which continued throughout the experiment in some samples. Enrichments in nitrite alone were delayed in some samples relative to the enrichments in TAN. The increase in nitrite in the control sample at ~25 days cannot presently be explained.

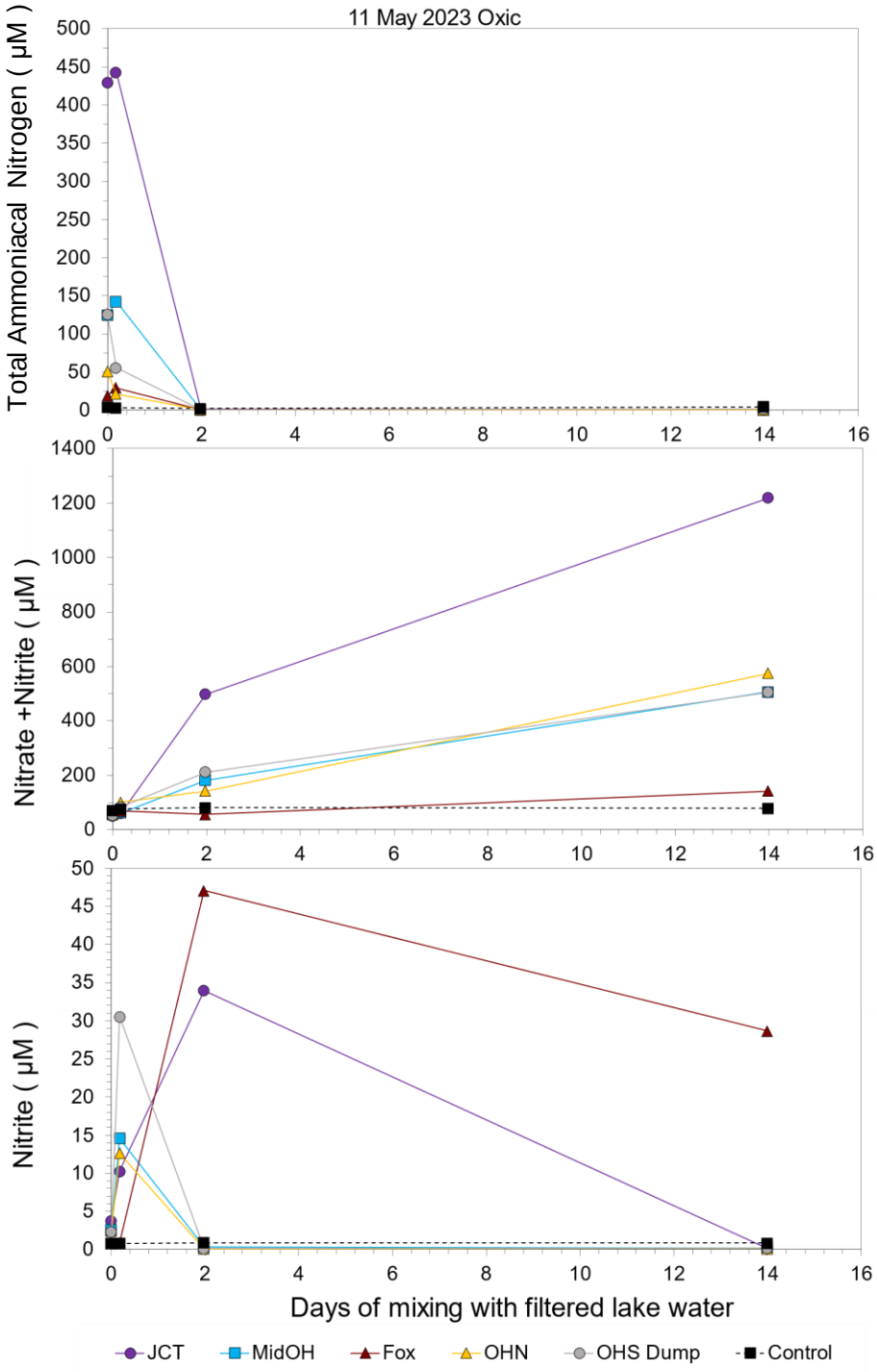


Figure 11: Dissolved inorganic nitrogen dynamics from the May 11, 2023 oxic porewater leaching experiment. In all samples, TAN concentrations dropped to low levels by 2 days, including MidOH which exhibited lingering TAN elevation up to 10 days in the previous June 25, 2022 experiment. This was accompanied by a rise in nitrate + nitrite, continuing throughout the entire experiment in most samples. Enrichments in nitrite alone were delayed in some samples relative to those for TAN.

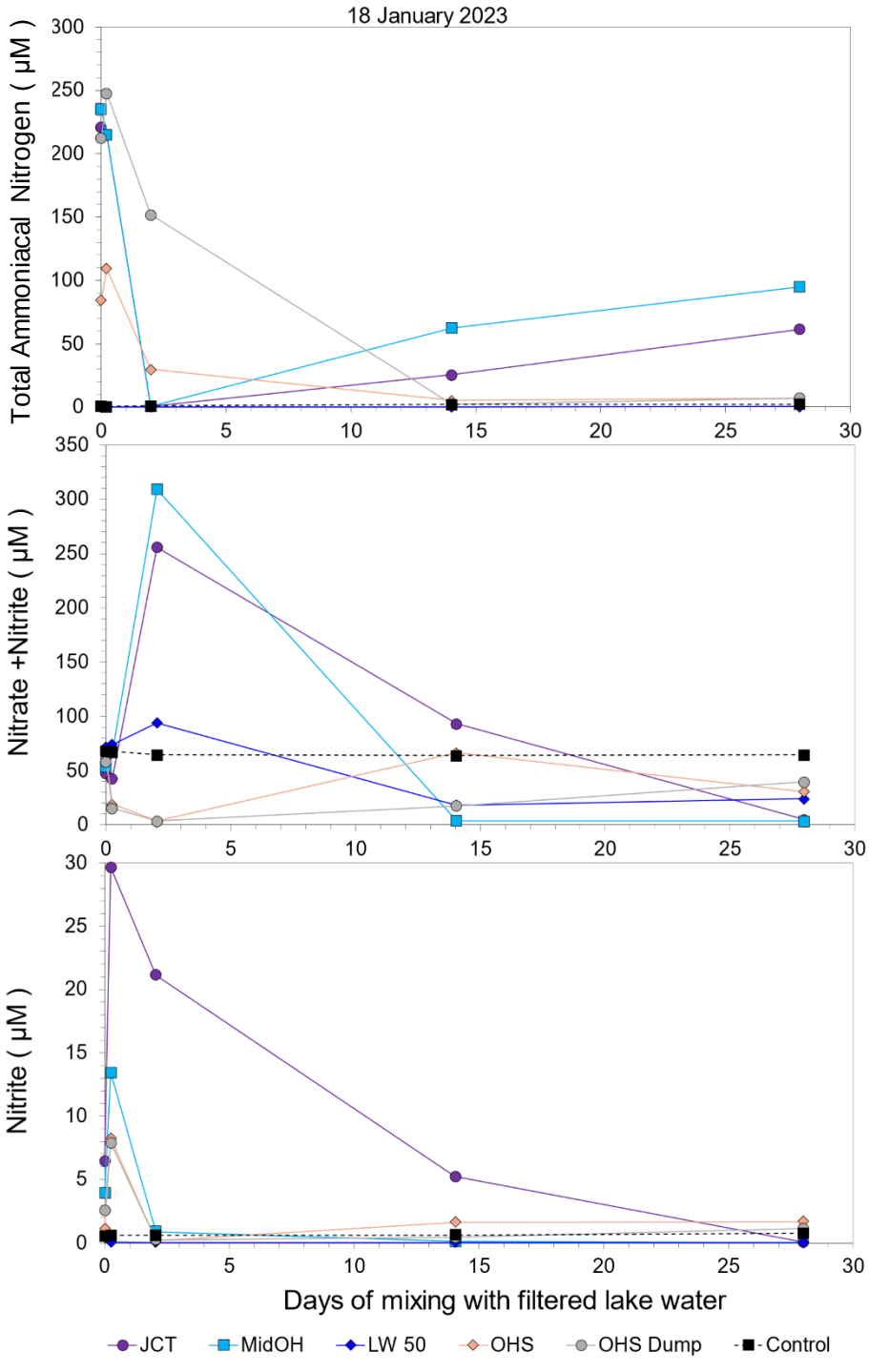


Figure 12: Dissolved inorganic nitrogen dynamics of the 18 January, 2023 porewater leaching experiment. Unlike the experiments previously discussed (Figures 10-11), some samples in this experiment experienced a gradual TAN increase over time with no initial enrichment, while nitrate in those same samples peaked at 2 days then lowered throughout the remainder of the experiment. This suggests that these samples may have experienced anoxic conditions during this experiment.

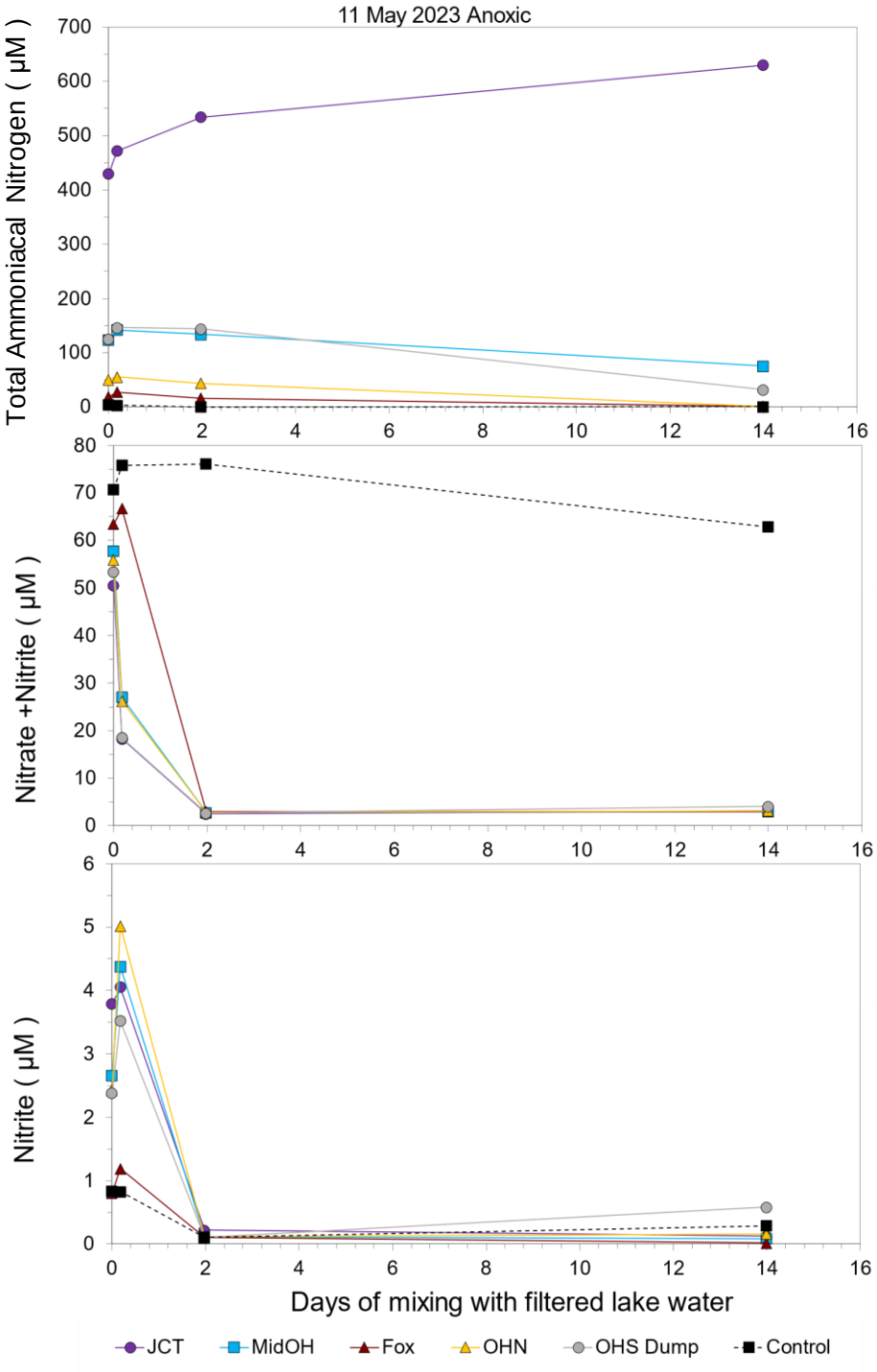


Figure 13: Inorganic nitrogen dynamics of the 11 May, 2023 anoxic porewater leaching experiment. TAN concentrations either remained constant or slowly increased over time, while nitrate and nitrite both peaked initially before dropping to low values, where they remained mostly constant through the remainder of the experiment.

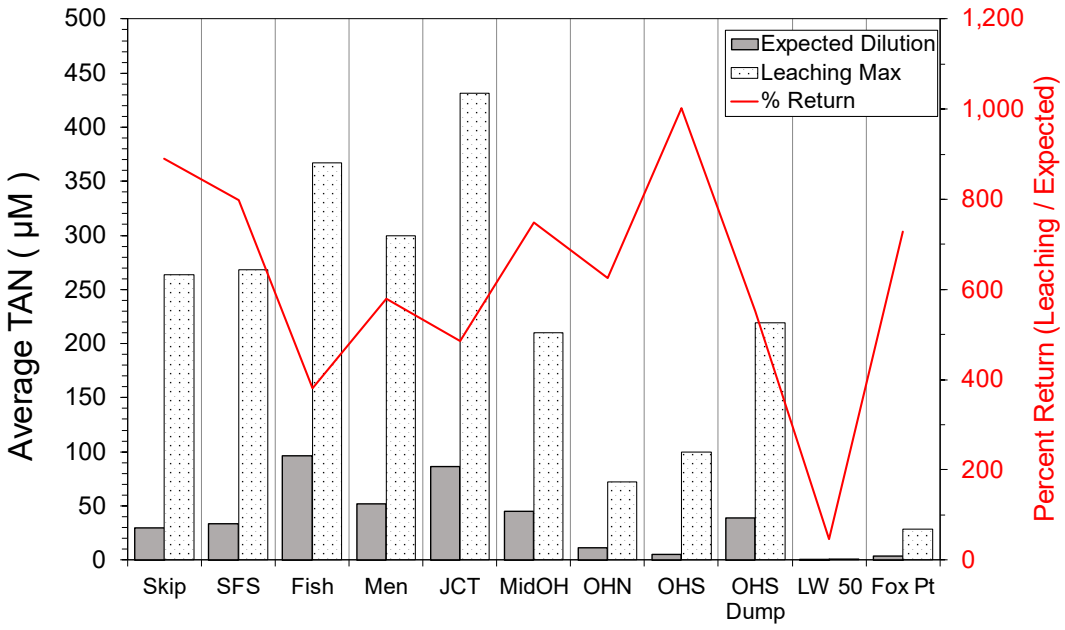


Figure 14: Observed vs. expected average TAN leachate concentration. Note that LW 50 is the only station without a large percent return, but with the expected and real leachate concentrations so low (0.05 and 0.02 µM, respectively, both below the limit of quantification) the discrepancy is not meaningful.

### 3.2.3 Dissolved Phosphorus

The soluble reactive phosphorus (SRP) contents of surface sediment porewaters varied significantly between the river and harbor stations, with harbor sediments and JCT showing very high concentrations (10-40 µM) relative to the overlying waters (typically < 1 µM) (Figure 15). The stations upriver of JCT were scarcely enriched at all over their respective water columns, with most stations < 3 µM except for FISH on 20 June, 2023. As for JCT itself, SRP was very highly elevated on 18 January and 11 May but was near detection limits on 25 July and 20 June. Combined with the high difference in SRP in the Fish samples between 25 July and 20 June, this suggests either some seasonal process greatly affecting the SRP contents of sediment porewaters in the Milwaukee River or some form of analytical error—sampling frequency of the river stations was too low to be certain. Harbor sediments were also more highly enriched in FP

compared to the river sediments as well as the corresponding water columns (Figure 16). In most samples, the difference between FP and SRP was less than 1 μM and less than 3 μM in all but OHS Dump, suggesting that there is very little non-bioavailable dissolved phosphorus in AOC porewaters. In the OHS dump porewater from 25 July, 2022, SRP was much higher than FP, which should not be possible given that FP includes SRP by definition. This may be an analytical error.

In the leaching experiments, SRP concentrations tended to increase rapidly in the first few hours after initial mixing. After that point, SRP would either continue to rise through the end of the experiment or level off at an apparent maximum, as was the case in the Fox and LW 50 samples (Figure 17). SRP leaching does not appear to have been significantly affected by the supposed development of anoxic conditions during the 18 January experiment. Like TAN, the SRP concentrations achieved in these experiments were much higher than those that would be expected based on a simple dilution of the sediment. Most samples reached concentrations approximately 2-8x higher than that expected based on the initial porewater concentrations (Figure 18). FP was not analyzed in the rolling experiments due to a lack of sample volume.

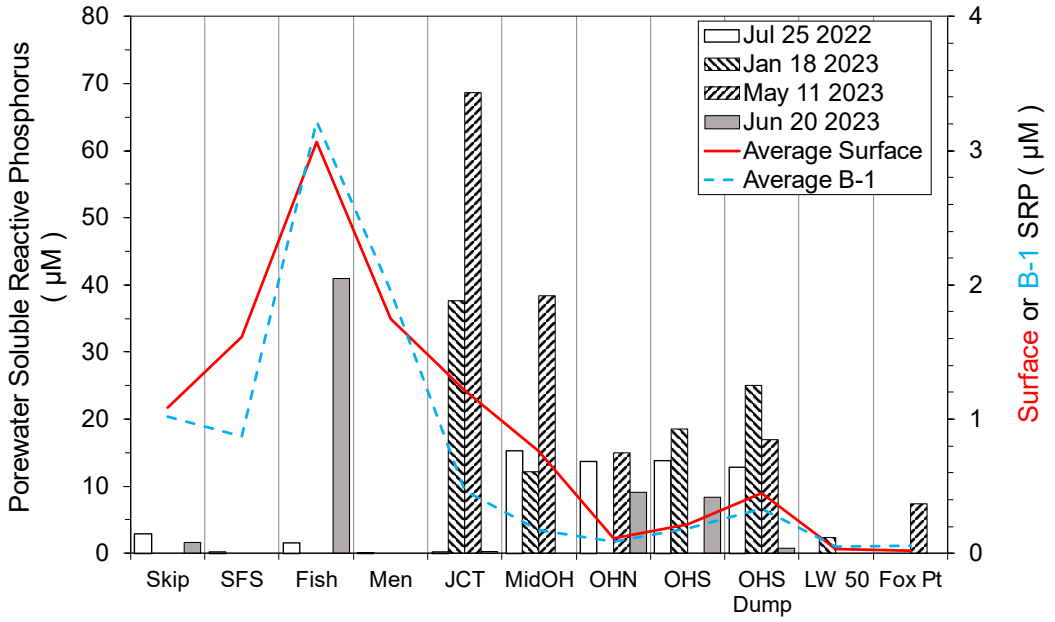


Figure 15: Soluble reactive phosphorus contents of surface sediment porewaters and their respective water column averages. Harbor and nearshore porewaters tended to be highly elevated over their water columns (> 10x) but river porewaters were elevated little if at all over their water columns.

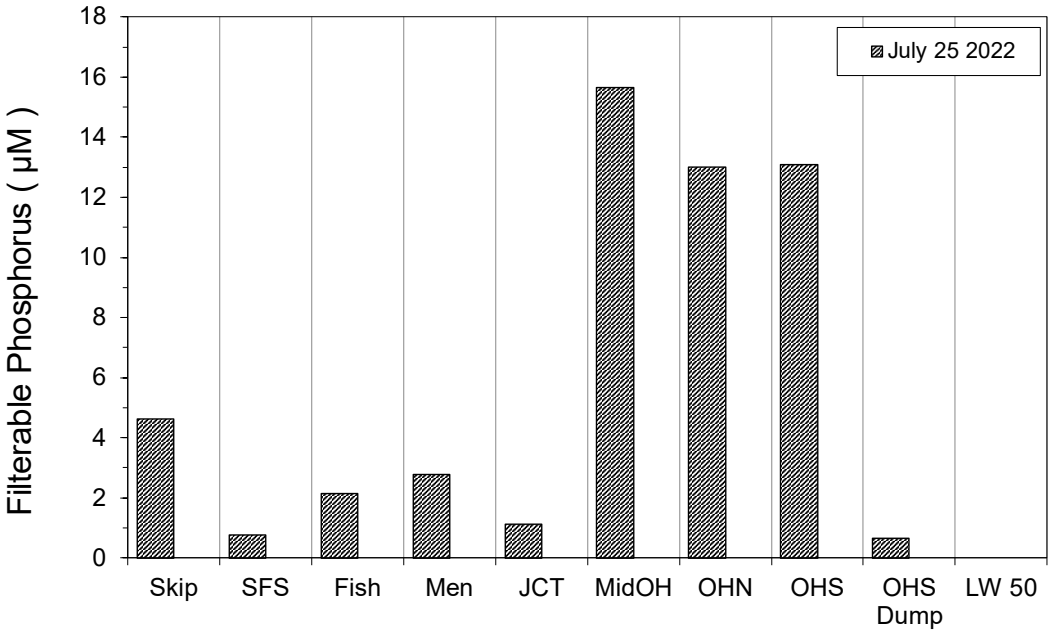


Figure 16: Filterable phosphorus contents of surface sediment porewaters.

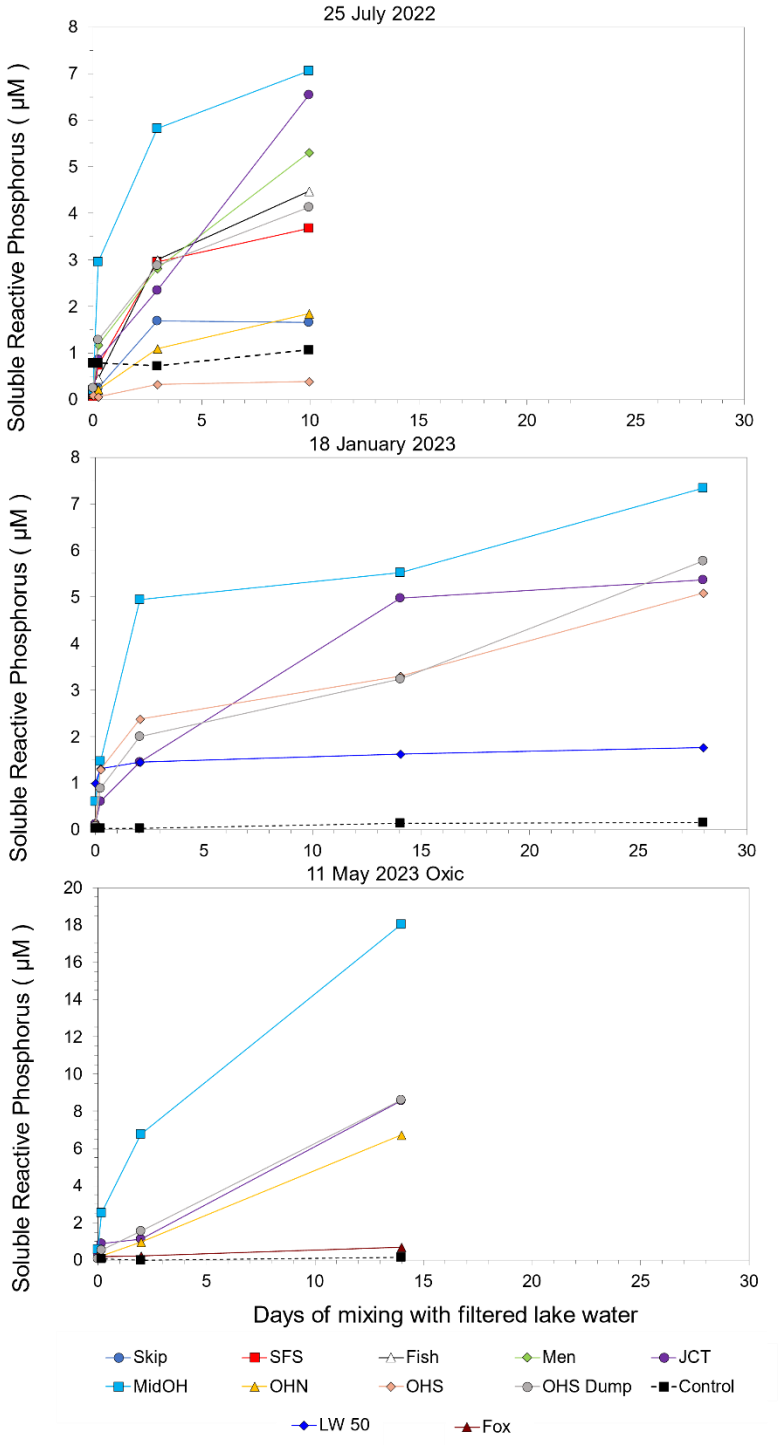


Figure 17: Soluble Reactive Phosphorus dynamics from the 25 July, 18 January, and 11 May oxic experiments. SRP was not measured in the anoxic 11 May experiment because of sample volume restrictions.

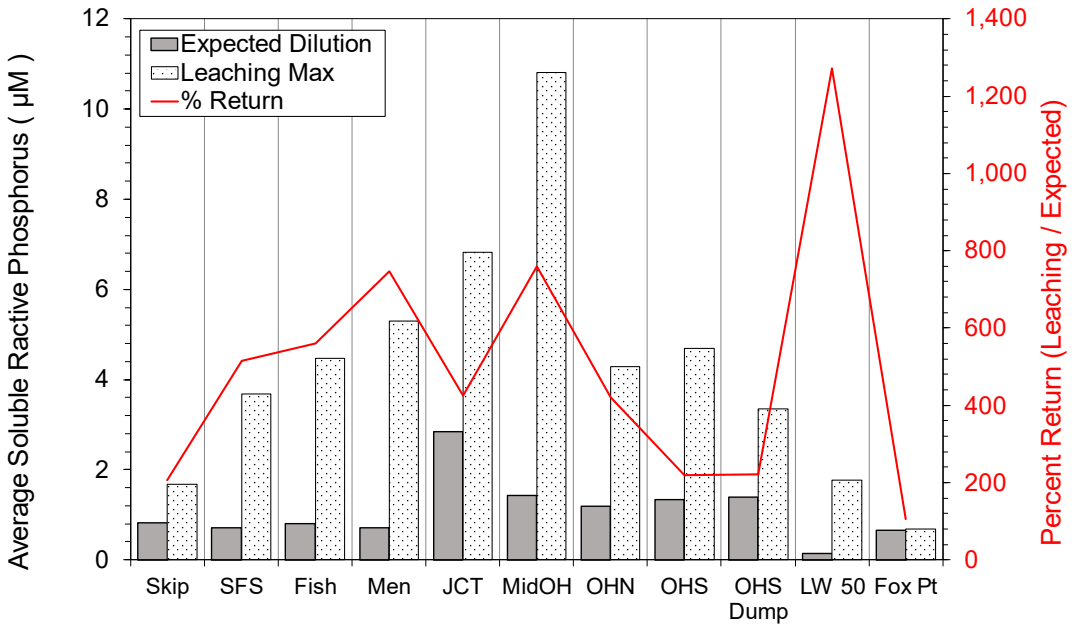


Figure 18: Observed vs. expected average SRP leachate concentration.

### 3.2.4 Dissolved Carbon

Most surface sediment samples were enriched in Dissolved Inorganic Carbon (DIC) compared to their corresponding water samples, especially at JCT (Figure 19). In general, the river sediment samples were more highly enriched in DIC relative to the waters above than the harbor samples, with the exception of OHS Dump which was more similar to the rivers in its DIC enrichment. LW50 and Fox Pt were only slightly enriched over their water columns. In all cases, there was no noticeable enrichment of DIC in the bottom waters over the surface waters.

Dissolved inorganic carbon dynamics were inconsistent between leaching experiments (Figure 20). In the 25 July experiment the river samples all exhibited an increase in DIC over time of approximately 50%. The harbor samples then began to decrease after reaching a maximum in about three days ($t_2$) before apparently remaining constant for the remainder of the experiment. In the 18 January experiment all samples increased over time with location of origin

driving the extent of the release. In the 11 May experiment all samples (including the control) decreased with time, in both oxic and anoxic sample sets. In the oxic set this could be explained by assuming that the frequent opening of the bottles to ensure adequate oxygen supply allowed gaseous $CO_2$ to escape from solution, but this would not be expected to occur in the anoxic experiment, which was carried out in sealed syringes that were only opened when sampling. This may be due to changes in the inorganic carbon equilibrium, which is discussed in more detail in section 4.4. Regardless of the specific dynamics, however, average DIC returns by the ends of the experiments were high in most samples—between 2-8x in the AOC samples (Figure 21). In the nearshore samples, DIC returns were approximately 13x higher than expected in LW 50 but were not elevated (100% return) at Fox Pt.

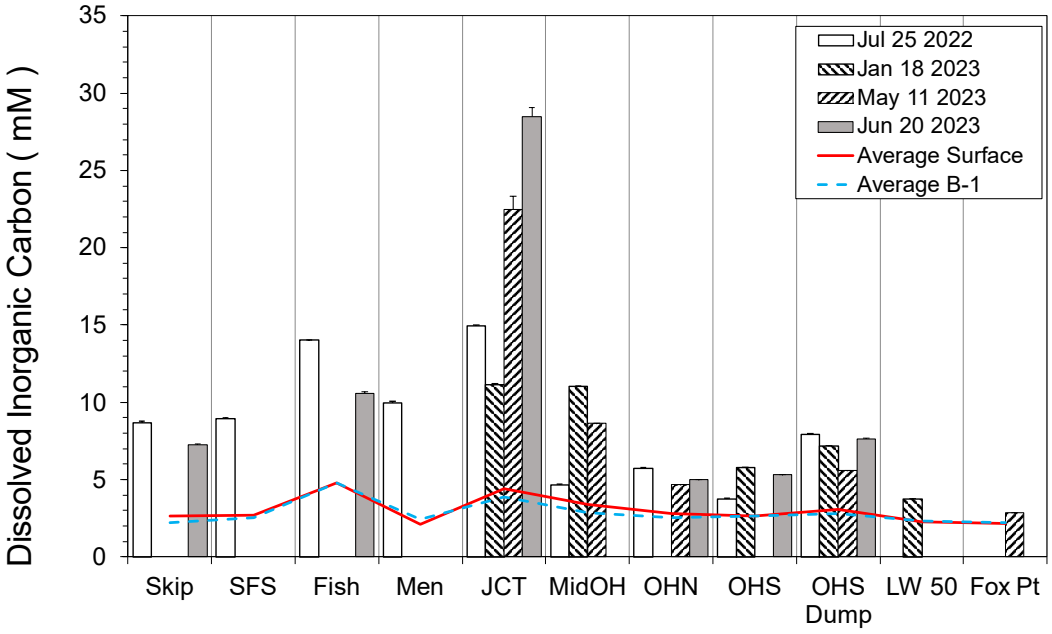


Figure 19: Dissolved inorganic carbon (DIC) contents of surface sediment porewaters compared to their corresponding water columns. Surface sediment porewaters were always higher in DIC than the overlying water.

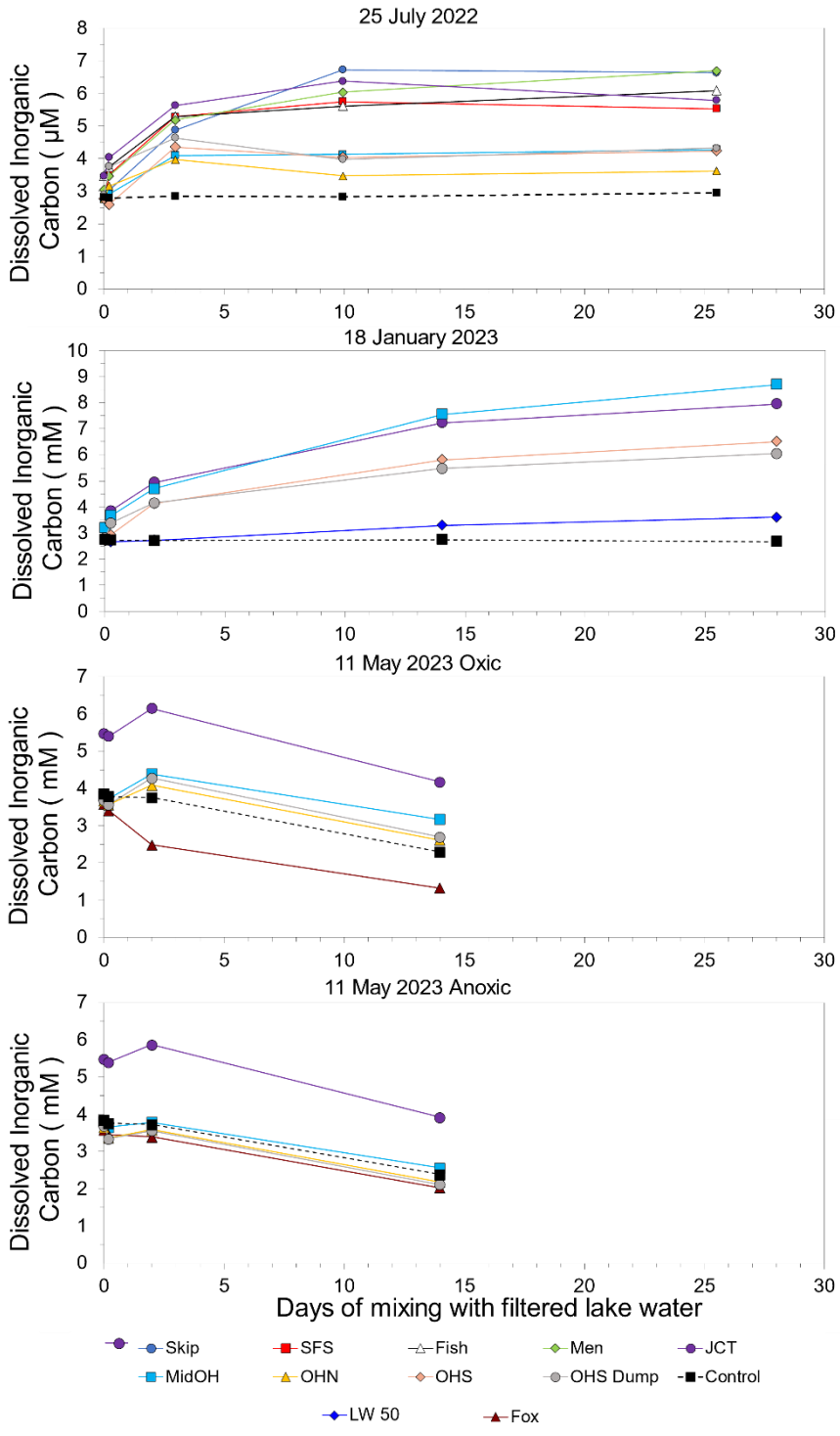


Figure 20: Dissolved inorganic carbon (DIC) dynamics from all four leaching experiments. In both experiments on 11 May, DIC decreased over time as opposed to the previous two experiments, where DIC either increased or stayed relatively constant depending on the sample.

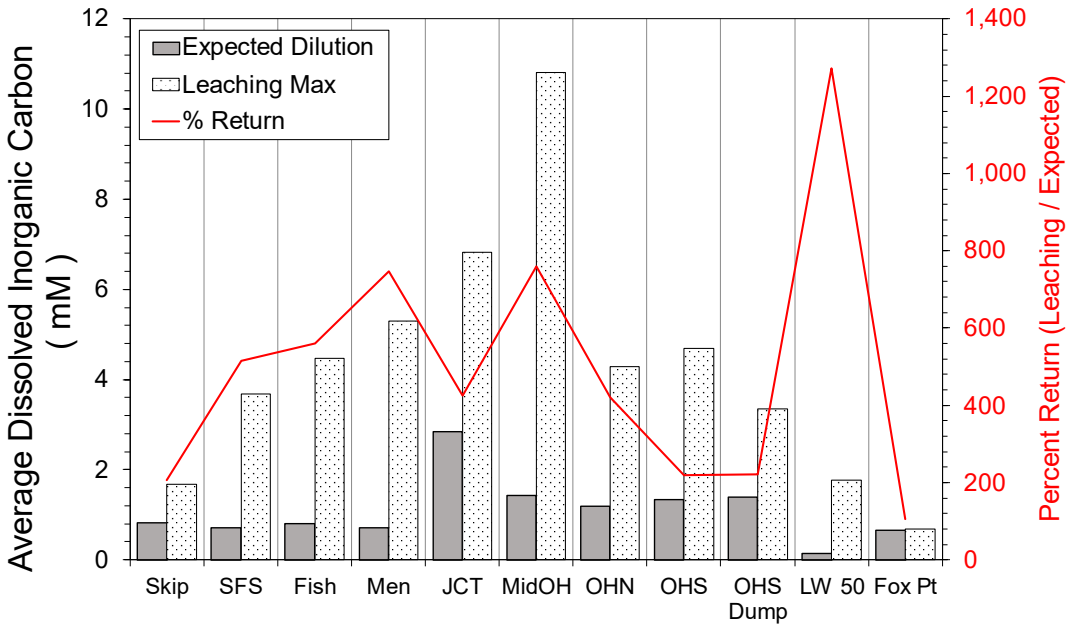


Figure 21: Observed vs. expected average DIC leachate concentration.

Porewaters also contained higher concentrations of dissolved organic carbon (DOC) than the overlying waters (Figure 22). However, they were not as highly enriched in DOC as DIC, with the former approximately 10x lower than the latter in all samples. DOC was measured in one leaching experiment (25 July 2022, Figure 23), and it demonstrated a slightly different temporal pattern than DIC. Most samples stayed at a nearly constant concentration throughout the experiment except for SKIP and MidOH, which both rose by about 0.8 mM over time.

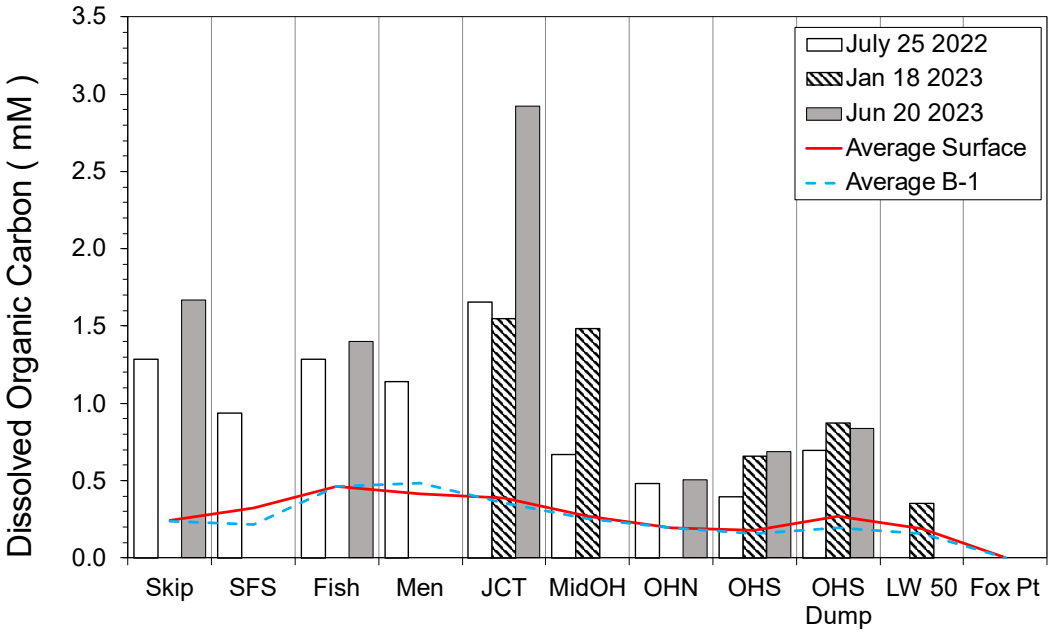


Figure 22: Dissolved organic carbon (DOC) contents of surface sediment porewaters compared to their water columns. Like DIC, surface sediment porewaters were always higher in DOC than the overlying water, though overall DOC concentrations in porewater were consistently about 10x lower than DIC. No DOC data are available for May 11, 2023.

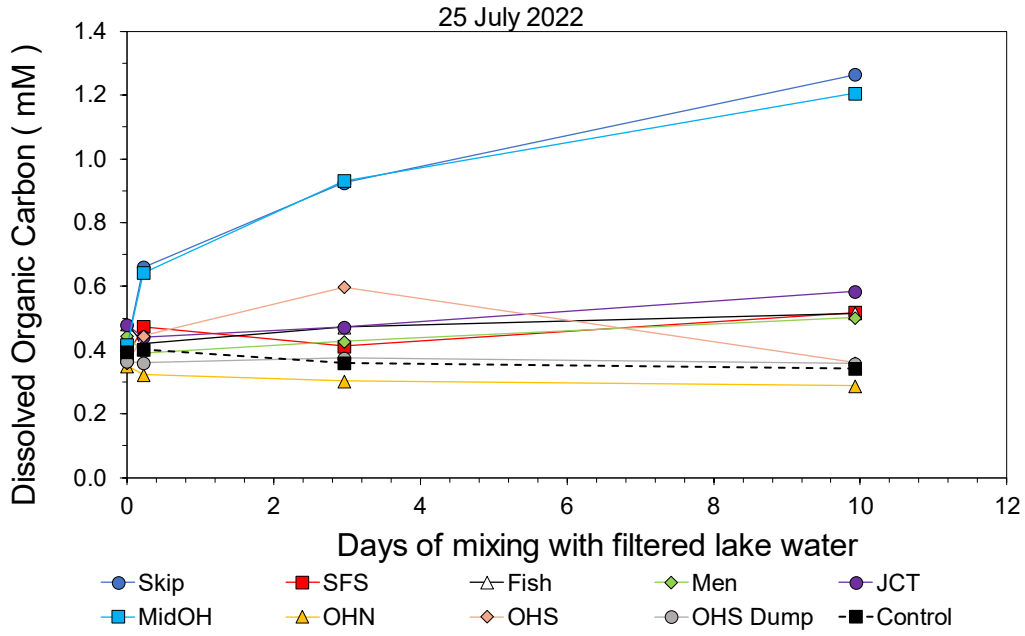


Figure 23: Dissolved organic carbon (DOC) dynamics from the 25 July, 2022 leaching experiment. This was the only leaching experiment in which DOC was measured due mostly to sample volume restrictions

# 4 DISCUSSION

## 4.1 Factors Affecting Nitrogen Dynamics

Dynamics among inorganic nitrogen species during the leaching experiments indicate activity of some biogeochemical process(es) beyond simple leaching into the water over time. Of particular interest is the relationship between TAN and nitrate, as the relative dynamics of the two are crucial to the viability and composition of algal blooms. Immediately, fixation of $N_2$ gas can be effectively eliminated as a likely biogeochemical process at play in the leaching experiments because nitrogen-fixing bacteria tend to only utilize $N_2$ in the absence of more energetically favorable forms of nitrogen, namely nitrate or ammoniacal nitrogen. Because nitrate and/or TAN were present in adequate concentrations during the leaching experiments, it is unlikely that nitrogen fixation occurred to any measurable extent.

At one location, MidOH on 20 June, 2023, there was a large TAN enrichment in the near-bottom water over the surface water—0.4 μM vs. 8.3 μM at the surface and bottom, respectively. This was not observed at any other point, and could possibly be explained by the concurrent dredging project that was occurring upriver from this station rather than by biogeochemical factors. If TAN were released into the rivers in the dredge plume, that enrichment would be expected to be most prevalent in the bottom waters. However, the fact that JCT is not similarly enriched may cast some doubt on this conclusion as it is also downriver of the dredging, and is closer to the dredged location.

### 4.1.1 Nitrification

In aquatic environments, DIN is converted among its different forms ($NO_3^-$, $NO_2^-$, $NH_3$, $NH_4^+$) by a combination of physical and biological processes. Ammoniacal nitrogen ($NH_3$ &

$NH_4^+$) will readily interconvert at neutral pH, hence why they are analyzed collectively as Total Ammoniacal Nitrogen (TAN). Nitrite is largely produced by ammonia-oxidizing bacteria (AOB) such as *Nitrosomonas* which derive energy from the reaction (Figure 24, top). For the most part, nitrate is produced from nitrite by nitrite-oxidizing bacteria (NOB) such as *Nitrobacter* that similarly derive energy from the reaction (Figure 24, bottom). These two half-reactions ($NH_3 \rightarrow NO_2^-$ by AOB and $NO_2^- \rightarrow NO_3^-$ by NOB) collectively result in the process of nitrification, in which ammoniacal nitrogen (AN) is transformed into nitrate [Ward 2013, Aguilar & Cuhel 2023]. Crucially, nitrification is an aerobic process, requiring the presence of oxygen. Nitrification will also increase the acidity of the environment as nitrogen is oxidized, as a net of two hydrogen ions are produced during the process—one from each half-reaction (Figure 24, top).

$$NH_3 \rightarrow [NH_2OH] \rightarrow HNO_2 \rightarrow H^+ + NO_2^-$$

$$NO_2^- + H_2O \rightarrow H^+ + HNO_3 \rightarrow H^+ + NO_3^-$$

Figure 24: Reaction scheme for the two-step process of nitrification [adapted from Aguilar & Cuhel 2023]. The top equation, or half-reaction, is performed by ammonia-oxidizing bacteria (AOB) and the bottom by nitrite-oxidizing bacteria (NOB).

In the oxic rolling experiments, the initial TAN maxima typically occurred at $t_1$, or approximately four hours after mixing. Also occurring at or near $t_1$ in most samples were noticeable "deficits" of nitrate when comparing the observed vs. expected concentrations at $t_1$ of the rolling experiments (Figure 25). By the end of the experiments ($t_3$), the return on nitrate had increased considerably (Figure 26). Furthermore, the initial TAN enrichment was always accompanied by a nitrite enrichment, though often the nitrite maxima lagged those of TAN between the $t_1$ and $t_2$ sampling points. These data strongly suggest nitrification converting AN into nitrate via nitrite as an intermediate. This would explain the deficit in nitrate at $t_1$ as TAN

was reaching its peak concentrations and nitrification had not yet substantially increased nitrate release relative to the receiving waters that already contained an appreciable concentration of nitrate (Figure 25). This is further reinforced by the near total depletion of TAN after $t_2$ approximately corresponding to the nitrite maxima (as expected of the intermediate product in complete nitrification) and the steady rise of nitrate throughout the experiments (as the nitrite is converted into nitrate) eventually reaching maxima at the end of the experiments, $t_3$ (Figure 26). However, the acidification that would normally be expected of active nitrification was not observed in the 25 July, 2022 leaching experiment—this is likely due to the high carbonate buffering capacity of the sediment porewaters (see section 4.4 for more detail).

To reiterate from section 2.4, the sediment leaching experiments were designed to approximate the conditions within the slurry transport pipe. If the pipeline is kept oxygenated, then it is likely that at least some AN present in the slurry will be nitrified into nitrate within the 4-5 hours transit time, though in the leaching experiments it took closer to 2 days for AN to be depleted completely. However, since the pipeline is pressurized, there will be no exchange of oxygen with the surrounding environment except at either end. This means that the dissolved oxygen in the water with which the slurry is initially made will be the only oxygen that is available for nitrification over the length of the pipeline. With an average dissolved oxygen gas ($O_2$) content of the AOC waters of about 300 μM (measured by sonde) and thus an O concentration of 600 μM, an average porewater AN concentration of 1000 μM, a 5x increase in AN on average due to decomposition by 4-5 hours, and a 1:1 mixture of water and sediment to make the slurry, the molar ratio of AN:O in the initial slurry (that is, the slurry just as it enters the transport pipeline) is approximately 4:1. This may result in an AN-enriched slurry being deposited at the CDF due to a relative deficit in oxygen compared to an abundance of AN.

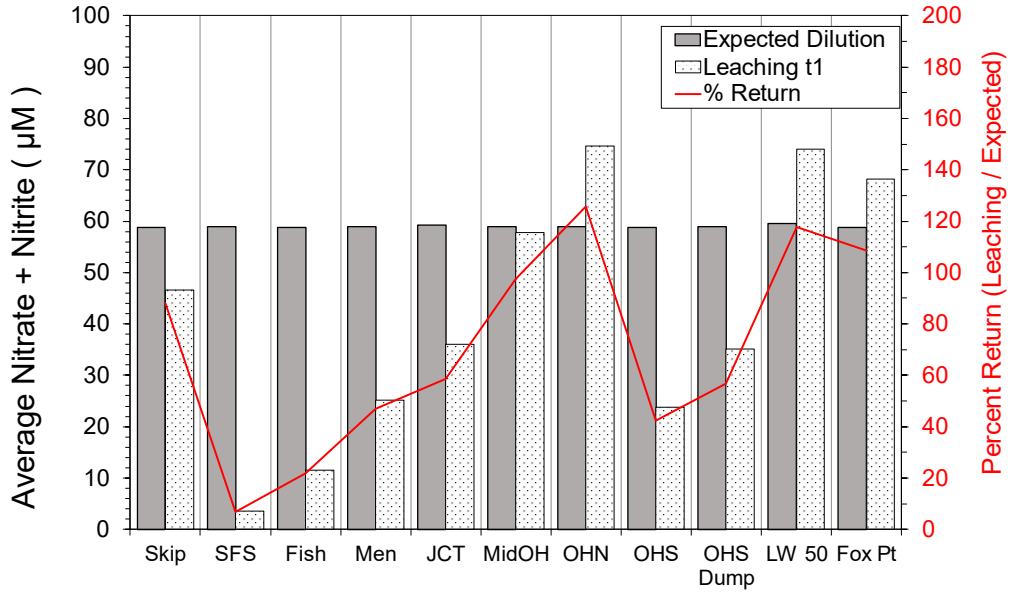


Figure 25: Observed vs. expected average nitrate + nitrite leachate concentration by $t_1$ of the leaching experiments. The return on nitrate + nitrite was almost always lower than expected (< 100%) by $t_1$. While this does coincide with TAN enrichments, this is likely not due to any biogeochemical ammonification processes but rather to the gradual production and release of nitrate over time. Note that the expected dilutions are all similar due to the high content in the receiving harbor water—higher than what was originally present in the porewater samples.

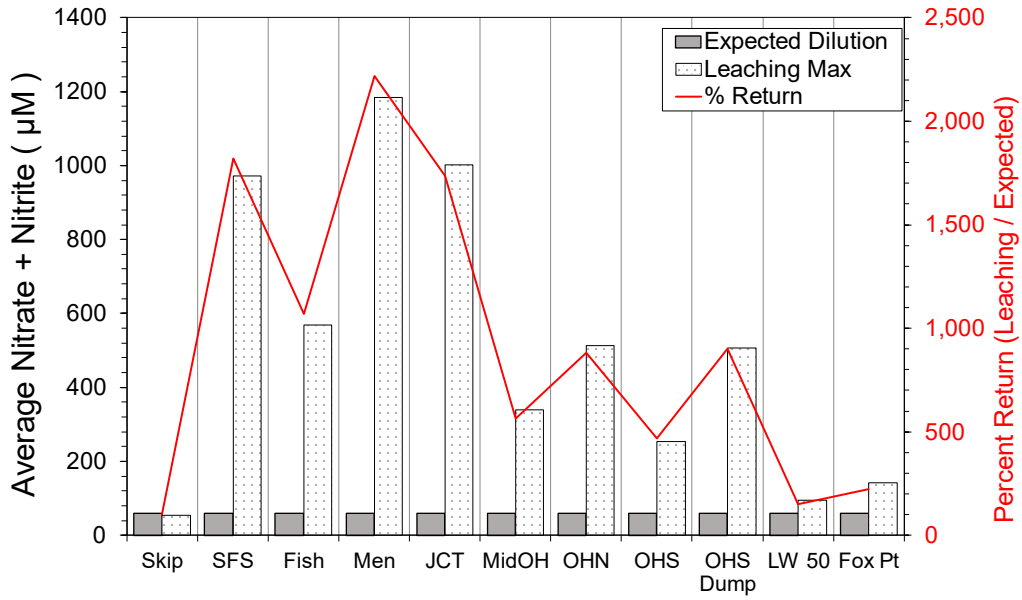


Figure 26: Observed vs. expected maximum average nitrate + nitrite leachate concentration. The leaching maxima were calculated using the $t_3$ values from each experiment, as opposed to the $t_1$ values used in Figure 25 which correspond with the TAN maxima. The return on nitrate + nitrite was almost always higher than expected.

### 4.1.2 Decomposition & Anaerobic Nitrogen Respiration

Dissolved oxygen does not penetrate downwards into sediments very far—usually one millimeter, at most [Jørgensen & Revsbech 1985]. This means that all sediment underneath this surface diffusive layer—whether it sedimented there naturally or was rapidly buried in a CDF—is anoxic. Nitrification does not occur in anoxic environments, but anaerobic bacteria can make use of nitrate as an alternate electron receptor. Anaerobic respiration of nitrate is one way in which nitrate is reduced back into other forms of inorganic nitrogen following nitrification. For the purposes of this study, there are two biological pathways of anaerobic nitrogen respiration: denitrification and dissimilatory nitrate reduction to ammonium (DNRA). In the former, bacteria transform nitrate into gaseous $N_2$, while in the latter nitrogen is further reduced to ammonium [Burgin 2007, Broman 2021]. Aside from anaerobic respiration, the decomposition of organic nitrogen is another process in which inorganic nitrogen can be introduced into an environment. Whether this be as reduced forms (AN) or oxidized forms (nitrate/nitrite) depends on the structure of the original molecules, though amines (such as the amino acids in proteins) tend to decompose into AN.

Returning to the leaching experiments, extremely high return in the initial TAN enrichments around $t_1$ suggest that there is additional AN being produced in or (released from) the sediment after it is disturbed and allowed to mix with the water. This AN production could be caused by two biological processes: decomposition of organic nitrogen and/or DNRA, with the former the more likely explanation due to the oxygenated conditions in the bottles. Organic decomposition is also likely the process most responsible for the high TAN content in the sediments in the first place, as it was shown that the sediment porewaters are also relatively high in DON, the available stock of which is likely to be regularly refreshed from the sedimentation

of particulate organic material out of the water column. Though particulate nutrients were not measured as part of this study, it is likely safe to assume that sediments are rich in particulate nutrients, especially in estuaries where nutrient-rich riverine water feeds the growth of large algal populations, which eventually die and deposit into the sediment as Particulate Organic Material (POM) [Brady 2013]. A constant supply of organic nitrogen leads to constant microbial decomposition in turn resulting in a constant production of AN which is buried in the sediment over time. Upon the initial mixing with water in the rolling experiments, dissolved AN is freed from porewater. This would contribute to the higher-than-expected return in the leaching experiment. It is also possible that the bacteria responsible for this decomposition benefitted not only from the sudden release of organic nitrogen but also the increased surface area from re-suspended POM. This may have further increased the rate of POM decomposition, subsequently increasing the TAN return.

## 4.2 Factors Affecting Phosphorus Dynamics

When oxygen is not abundant enough for aerobic respiration, facultative anaerobic bacteria will begin anaerobic respiration with the next highest redox potential—that is, the electron receptor that is most energetically favorable—after oxygen. In anaerobic sediments, these alternative forms of respiration can account for many observed chemical dynamics. As described in section 4.1, the most energetically favorable (and commonly utilized) non-oxygen electron acceptor is nitrate. This partially explains why anaerobic nitrogen reduction processes (like DNRA or denitrification) tend to reliably occur even in sediments that have only been anoxic for a short time given that adequate $NO_3^-$ is present, and thusly tend to be major components of overall nitrogen dynamics at the SWI.

Phosphorus has a very low redox potential, meaning that phosphorus makes for a very energetically unfavorable electron receptor. This results in geochemical or indirectly-coupled biochemical processes playing much larger roles in phosphorus dynamics at the SWI. As the limiting nutrient for algal growth in Lake Michigan, it is normally present in small concentrations (< 0.1 μM) in the water column, making the potential for the sudden introduction of large quantities of bioavailable SRP from dredged sediments concerning.

The high return on SRP during the leaching experiments (Figure 18) implies that there is a net-source of labile phosphorus within the sediments. One source of this SRP is likely microbial POM decomposition—just as the decomposition of organic nitrogen leads to an increase in dissolved nitrogen, so too does the decomposition of organic phosphorus lead to an increase in dissolved phosphorus. Also like nitrogen, organic decomposition is likely the main source of the high SRP content of the initial porewaters by similar logic.

There is also the conversion of Particulate Inorganic Phosphorus (PIP) to SRP by geochemical processes to consider. Orthophosphate can adhere to carbonate particles that can deposit into sediments [Brooks & Edgington 1994]. The favorability of the formation of these complexes depends partly on pH, and in an environment experiencing gradual acidification due to nitrification the dissociation of carbonate-phosphate particles may be a possible source of SRP that, when coupled with the buffering capacity of the inorganic carbon equilibrium, may result in additional release of SRP without any accompanying changes in pH. Further discussion of this process requires first discussing the carbon dynamics observed in the leaching experiments, and thus is saved for section 4.4.

## 4.3 Nutrient Ratios of Porewater and Leaching Effluent

In surface sediment porewaters, N:P ratios (calculated using only DIN and SRP, as the bioavailable forms of those nutrients) were significantly higher in the rivers on 25 July than any other stations or times, between 250 and 9000 (Figure 27). However, these extreme values were not observed in any samples on either 18 January or 11 May. Most notably JCT (a river sample) had a highly elevated DIN:SRP ratio on 25 July but did not on either 18 January or 11 May. Ratios in the harbor and nearshore stations never rose above 150. The differences in DIN:SRP among stations may reflect systematic differences in the composition of sedimented organic material, as different biochemical compounds incorporate varying amounts of nitrogen and phosphorus. By $t_1$, the average DIN:SRP ratio rose (relative to the harbor stations) to 488.0, likely a representation of the larger TAN enrichment due to decomposition than SRP, and the extreme variation in DIN:SRP seen in the porewaters over the entire estuary was greatly reduced (Figure 28, top). By $t_3$, the average N:P ratio dropped down to 75.8—still elevated over the porewaters, but not nearly as much as was seen in $t_1$, perhaps due to the continued increase in SRP over time compared to a slowed DIN release (Figure 28, bottom).

Looking at ammoniacal nitrogen specifically instead of DIN gives slightly lower AN:SRP ratios in both porewater and $t_1$ samples (harbor averages of 28.7 and 373, with river porewaters from June 25 similarly between 250-9000) due to the relatively small nitrate and nitrite contents in those samples compared to AN. In the $t_3$ samples, however, AN:SRP ratios are all less than 10, with most less than 1 due to the depletion of AN by nitrification, meaning that SRP is more abundant than AN in those samples (Figure 29). Normal AN:SRP ratios in the outer harbor are around 2-4. The AN:SRP ratio is of particular interest as it was the high AN content in

dredging effluent that was suspected to have led to the toxic Cyanobacterial bloom in the inland lake described in section 1.4.

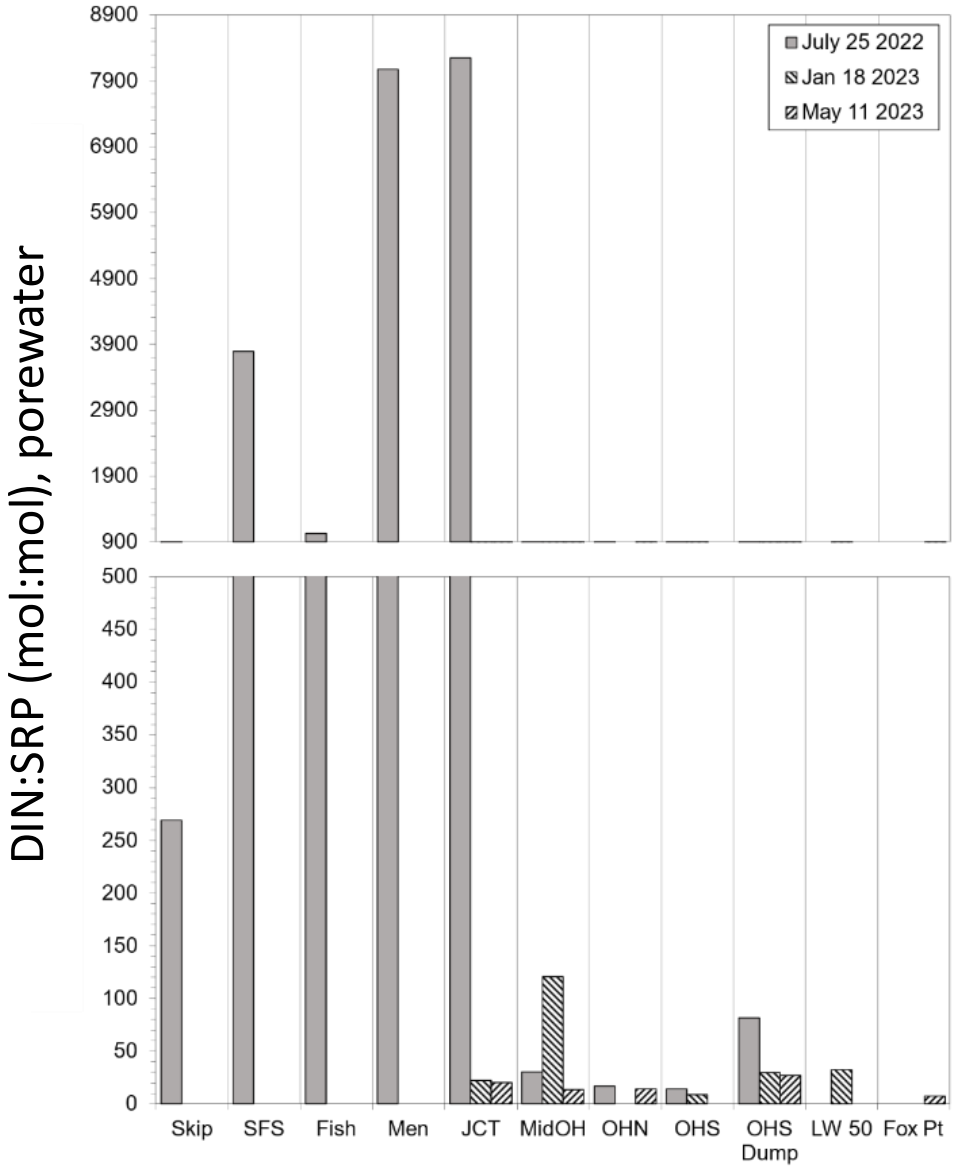


Figure 27: Bioavailable DIN:SRP ratios in surface sediment porewaters.

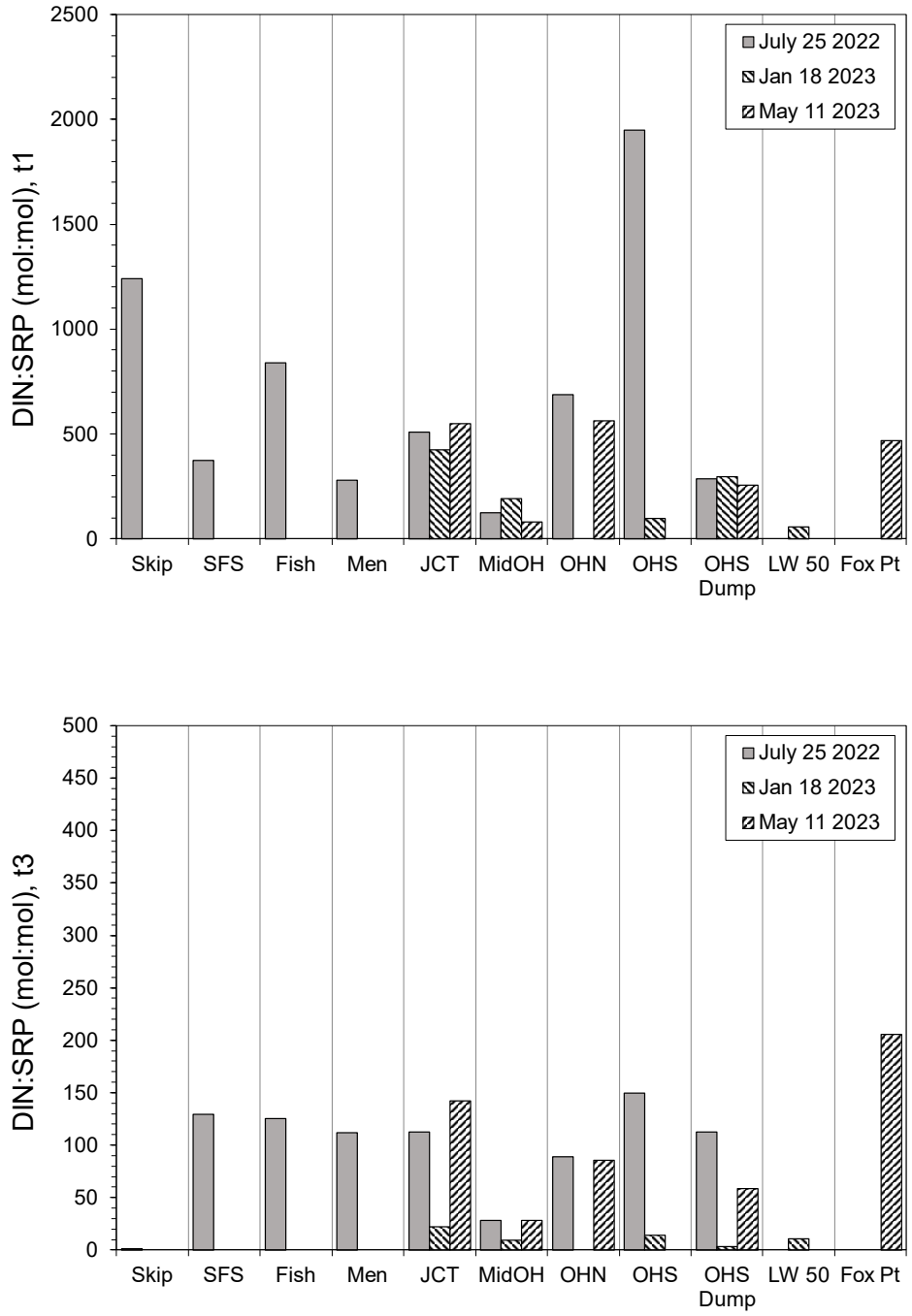


Figure 28: Bioavailable DIN:SRP ratios at $t_1$ (top) and $t_3$ (bottom) time points during leaching experiments.

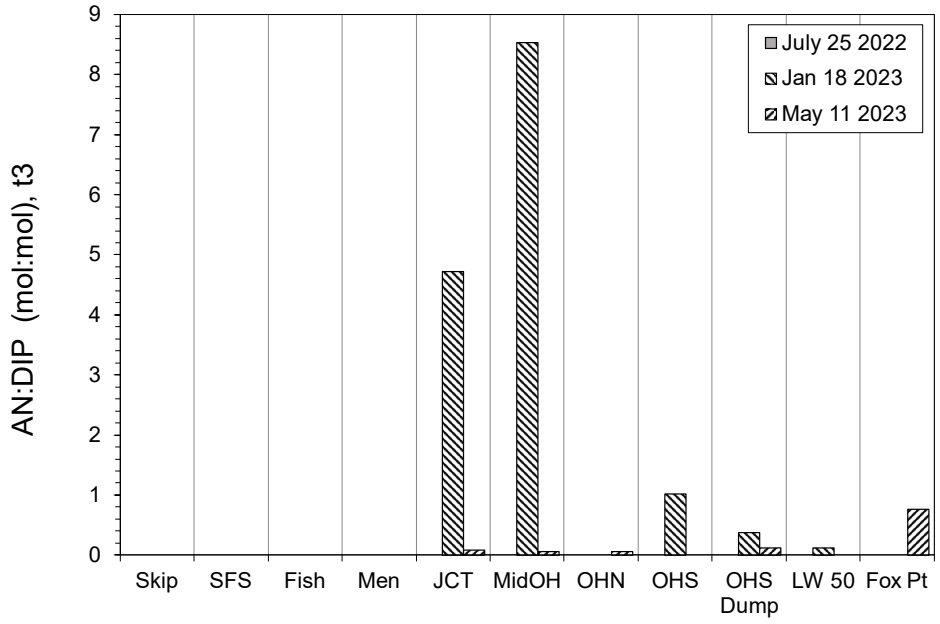


Figure 29: Ammoniacal nitrogen to SRP ratio at the $t_3$ time point during the leaching experiments. By $t_3$, many samples had AN contents at or below the limit of quantification, hence why the AN:SRP ratios appear to be 0.

## 4.4 Effects of Carbon Dynamics

Dissolved Inorganic Carbon (DIC) exists in equilibrium between four forms. From most to least reduced, these are carbon dioxide ($CO_2$), carbonic acid ($H_2CO_3$), bicarbonate ($HCO_3^-$), and carbonate ($CO_3^-$). This equilibrium is shown in Figure 30, scheme B. The relative dominance of these forms is determined by the pH of the solution. In neutral pH conditions (such as Lake Michigan, or the leaching experiments) the dominant form of inorganic carbon is bicarbonate. This equilibrium acts as a pH buffer, allowing the solution to resist large changes in pH. Carbonate buffering is largely responsible for Lake Michigan's relatively constant neutral pH, where the limestone-rich lakebed contributes plenty of calcium and magnesium carbonate ($CaCO_3$ and $MgCO_3$, respectively), and by extension carbonate, to the buffering capacity of the

water. In all likelihood this is true of the constant, neutral pH maintained in the leaching experiments as well, as they were carried out with sediment from Lake Michigan or its tributary rivers.

Though DIC is not a eutrophicating nutrient and will not contribute directly to the risk of unintentional algal blooms in the Milwaukee harbor, its release into the water may have indirect effects that could potentially exacerbate any eutrophication of the harbor through geochemical processes, largely through shifts in the carbonate equilibrium and any coupled biogeochemical processes. One of these effects may be the release of SRP through the dissolution of carbonate-phosphate particles. As mentioned in section 4.2, SRP can adhere to carbonate particles, forming particulate inorganic phosphorus (PIP) which will deposit in the sediment. When the environment becomes more acidic due to processes such as nitrification (Figure 30, scheme A), the carbonate in these particles will transform into gaseous $CO_2$—the same principle by which the flow-injection analysis method for DIC operates. A shift in the carbonate equilibrium towards $CO_2$-dominance necessitates a proportional reaction regenerating the concentration of carbonate and bicarbonate. This results in the dissociation of calcium (or magnesium) carbonate particles (Figure 30, scheme C). These particles can have phosphate adhered to them as PIP, and when the particles dissociate this PIP is released as SRP (Figure 30, scheme D). The carbonate bedrock of Lake Michigan contributes a high carbonate buffering capacity, that likely would not occur in unbuffered aquatic environments, such as in lakes with bedrock primarily composed of granite. In the leaching experiments, DIC concentration increased significantly over initial porewater contents, mostly likely due to decomposition by the same logic as was used in the nitrogen and phosphorus discussions. It may also be that the sediments are already rich in calcium carbonate, and the dissolution of $CaCO_3$ particles as described above further increased

DIC returns. This increase in DIC likely increased the already substantial buffering capacity of the receiving waters (Lake Michigan normally has about 2 mM DIC, with the outer harbor slightly higher) making it so only large changes in acidity or alkalinity could change the pH of the solution.

Additionally, the bicarbonate alkalinity of the receiving water may play a more direct role in the release of SRP from PIP, as it has been demonstrated that increasing alkalinity in the waters above organic-rich sediments can increase SRP concentrations [Lamers 2002, Smolders 2006]. In the case of the leaching experiments here, this could mean that as the concentration of DIC increases over time, the alkalinity increases, and more SRP is freed from particulate forms.

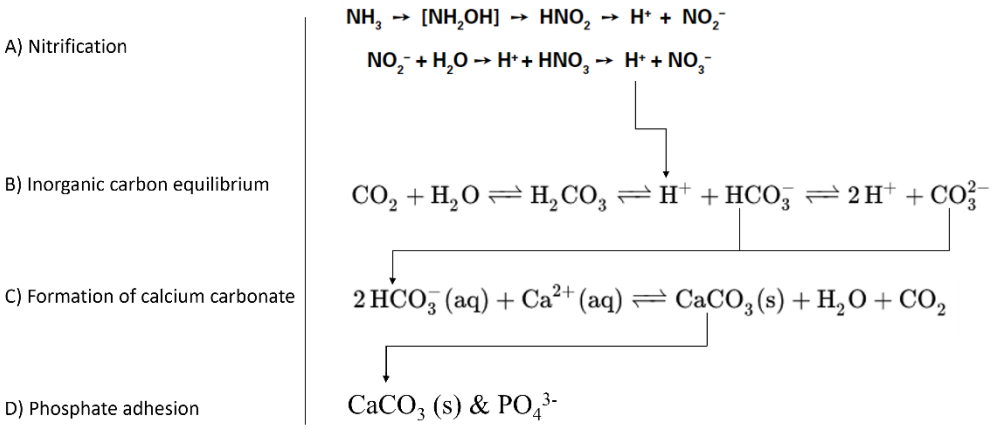


Figure 30: Reaction schemes for the adhesion of phosphate to carbonate particles as particulate inorganic phosphorus (PIP) and their subsequent release as soluble reactive phosphorus (SRP) in acidic conditions. A) Nitrification produces a net of two hydrogen ions, increasing the acidity of the solution [adapted from Aguilar & Cuhel 2023]. B). In acidic conditions, the dominant form of carbon in the inorganic carbon equilibrium shifts from bicarbonate ($HCO_3^-$) to carbon dioxide ($CO_2$) [adapted from Garrels & Christ 1965]. C) Bicarbonate and carbonate ($CO_3^{2-}$) ions can bind with calcium ions ($Ca^+$) to form calcium carbonate ($CaCO_3$), which precipitates out of solution in neutral conditions. In acidic conditions, calcium carbonate will dissociate [adapted from Garrels & Christ 1965]. D) Phosphate can adhere to the surface of $CaCO_3$ particles, forming PIP. When those particles dissociate under acidic conditions, any adhering phosphate is dissolved as SRP.

# 5 CONCLUSION

## 5.1 Eutrophicating Potential of Dredging in Milwaukee

Determining the eutrophicating potential of dredge plumes and dewatering effluents is not as simple as measuring the dissolved nutrient contents of the material to be dredged. Sediments are sites of complex nutrient dynamics driven by myriad biogeochemical processes that affect the release of nutrients during dredging-related disturbances. More than the initial nutrients content of the sediments, these biogeochemical processes determine not only the quantity of nutrients released but also in what forms they are released. This latter point is one component in estimating the risk of causing unseasonable algal blooms in the Milwaukee harbor due to dredging activity.

Dissolved nitrogen and phosphorus contents of sediment porewaters in the Milwaukee estuary AOC are far higher than what is found in the overlying waters, though this is not true of all forms of dissolved inorganic nitrogen (DIN). Ammoniacal nitrogen (AN) and soluble reactive phosphorus (SRP) comprise the bulk of the total dissolved nitrogen and phosphorus contents found in sediment porewaters. These are the forms of nitrogen and phosphorus, respectively, that are most readily bioavailable to algae. Sediments are also rich in organic matter, which is normally slowly decomposed by bacteria, gradually releasing nutrients into the porewater. When disturbed by dredging, these bacteria may increase decomposition due not only to an influx of oxygen but also the expansion of available surface area on which to attach themselves to suspended particulate organic matter (POM). This increased decomposition results in considerably more AN and SRP being released into the surrounding water following a

disturbance than was initially present in the sediment, but only lasts until the temporarily resuspended material can settle again.

The fate of porewater nutrients during and after dredging depends on the dredging method employed. Since a combination of mechanical and hydraulic methods is planned to be used to dredge the Milwaukee estuary, predictions regarding both are proposed. In the case of mechanical dredging, it seems likely that nutrients immediately freed from the sediments in this way will disperse into the surrounding waters. Since the waters are well-oxygenated, ammoniacal nitrogen will likely be transformed into nitrate by nitrifying bacteria within 4-5 hours of disturbance. The resulting acidification will not be measurable due to the high carbonate buffering capacity of the water but may nonetheless lead to the release of additional SRP due to the dissolution of carbonate-bound particulate inorganic phosphorus (PIP) via shifts in the carbonate equilibrium. Most of this nitrate and SRP will disperse through the water column until assimilated by algae or as far as stratification allows. In the rivers, which are generally well-mixed between December and April, they could reach the surface. The harbor is stratified throughout much of the year, so it may be that these nutrients will remain available only to hypolimnetic algae. They may circulate up to the surface when stratification weakens seasonally. Freed nutrients may otherwise flow out of the harbor into Lake Michigan; however, depending on the localized hydrodynamics immediately surrounding the dredging activity or DMMF, the residence time of discharge effluent in the harbor may be significantly different than the 3.1 day average observed for the entire outer harbor. Removed sediment will eventually be transferred to the DMMF, likely with most of the removed porewater still present unless a significant amount of time has passed. While the effects of dredge plumes may be expected to affect mainly the near-bottom waters in stratified conditions, relocation of the sediment (including transfer to and

from a holding barge) may also involve incidental re-introduction of removed sediments to the surface waters.

In the case of hydraulic dredging, dredge plumes will be smaller than those created by mechanical dredging. While these plumes will still result in nutrient release as described above, biogeochemical processes within the slurry transport pipeline will determine the nutrient content of the bulk of the removed sediments. Transport through the pipeline will subject the slurry to hypoxic or anoxic conditions during much of the transport due to the only source of oxygen being the water initially used to create the slurry. Anoxic conditions will prevent extensive nitrification from occurring before the material reaches the DMMF. Thus, the slurry deposited in the DMMF at the other end of the pipe will likely be highly enriched in both AN and SRP, more so than material removed by mechanical dredging. Relatively little additional SRP sourced from PIP dissolution is expected due to the lack of nitrification-induced acidification, though plenty will likely still result from decomposition. As nutrient-rich slurry is deposited in the CDF, this may result in a nutrient-rich effluent accumulating above the confined material. The faster rate of sediment removal provided by hydraulic dredging may mean that this material will be quickly buried by incoming material. Mixing sediments with water to create a slurry also means that effluent will accumulate in the DMMF faster, resulting in less time between the material's arrival in the DMMF and the nutrient-rich effluent being discharged into the harbor. There may not be enough time for nitrification to occur in the CDF, which would result in high concentrations of AN instead of nitrate in the discharged effluent. If the rate of dredging is slow enough, it is possible that the retention time of effluent in the CDF may be long enough to allow for nitrification to occur utilizing oxygen infiltration from the atmosphere. This depends both on the rate at which dredging is proceeding as well as internal hydrodynamics of the CDF thoroughly

circulating (and therefore oxygenating) the effluent, neither of which may occur. At the time of writing, treatment of effluent is included in the construction plans for the DMMF [WEC 2020], though the nature of this treatment has not been established.

## 5.2 Future Work

The work described here is the first part of the ongoing project to study the chemical and biological effects of dredging in the Milwaukee estuary, which will continue as dredging begins as scheduled in 2025. While the foundational chemical information necessary for this ongoing project is established here, some important knowledge gaps remain.

Firstly, this study focused entirely on the chemistry of surface sediments—approximately the top three centimeters that can be collected by PONAR. However, sediments up to three meters deep are going to be removed during the dredging process. Changes in temperature and the prevalence of anoxic conditions in lower layers of sediment are known to affect both the chemical content of deeper sediments and the biogeochemical processes that occur there [de Klein 2017, Shen 2023]. A study of sediment nutrient profiles within the AOC is necessary to address how the different chemical character of deeper sediments [perhaps using methods similar to Janke 1988] will affect the conclusions reached in this work, especially if most of the total volume of sediments to be removed are found below that which can be sampled via PONAR.

Additionally, many questions remain as to nutrient dynamics within the CDF. These dynamics may significantly alter the nutrient composition of discharged effluent but cannot be studied until the DMMF in Milwaukee is built. At the time of writing, construction is scheduled to begin in 2024. Similarly, the effects of benthic organisms on nutrient fluxes across the SWI [e.g. Turek 2015, Benelli 2018] may also warrant further investigation as they relate to dredging, as the work described here was done in the absence of any influences by benthic organisms

which is not representative of environmental conditions in the Milwaukee estuary. By the same logic, there are many biogeochemical nutrient dynamics that are coupled to metal dynamics that affect nutrient cycling both in surface waters and in sediments. Given the high metals content of the surface sediments (mostly solid-phase metals, see Table 2), these cannot be dismissed without study. Lastly, there are competing fates of nutrients in the outer harbor to consider. While the harbor does support a large algal population, this does not ensure that all nutrient enrichment of the harbor (from dredging or otherwise) will be assimilated by algae. There are other fates for these nutrients, both biogeochemical and hydrological, that are at play.

Perhaps most important is the continued study of algal growth in the harbor as an ecological phenomenon, as the success and distribution (spatially and temporally) of algal blooms is determined by many more factors than nutrient chemistry alone. These factors include the hydro- and thermo-dynamics of the harbor and the competing biology of different types of algae, as well as the chemical factors affecting nutrient availability. The focus of this study was chemistry, but moving forward the work on this project must eventually, necessarily, incorporate these other disciplines before a conclusion as to the eutrophicating potential of dredging in Milwaukee can be reached.

# 6 REFERENCES


Aguilar C & Cuhel R. (2023). Water quality and its relationship to freshwater recirculating aquaculture systems: An aquaculture technical brief. Published August 2023, University of Wisconsin Sea Grant Institute.

Benelli S, et al. (2017). Microphytobenthos and chironomid larvae attenuate nutrient recycling in shallow water sediments. *Freshwater Biology*. 63, 187-201. DOI: 10.1111/fwb.1305

Blomqvist P, Pettersson A, Hyenstrand P. (1994). Ammonium-nitrogen: A key regulatory factor causing dominance of non-nitrogen-fixing Cyanobacteria in aquatic systems. *Archiv für Hydrobiologie.* 132(2), 141-164. DOI: 10.1127/archiv-hydrobiol/132/1994/141

Boulton A, Datry T, Kasahara T, Mutz M, Stanford J. (2010). Ecology and management of the hyporheic zone: stream-groundwater interactions of running waters and their floodplains. *Journal of the North American Benthological Society*. 29(1), 26-40. DOI: 10.1899/08-017.1

Boyett, M. Tavakkoli A, Sobolev D. (2013). Mathematical modeling of competition for ammonium among bacteria, archaea, and Cyanobacteria within Cyanobacterial mats: Can ammonia-oxidizers force nitrogen fixation?. *Ocean Science Journal.* 48(3), 267-277. DOI: 10.1007/s12601-013-0025-y

Bradshaw C, et al. (2021). Physical disturbance by bottom trawling suspends particulate matter and alters biogeochemical processes on and near the seafloor. *Frontiers in Marine Science.* 8, 683331. DOI: 10.3389/fmars.2021.683331

Brady D, Testa J, Di Toro D, Boynton R, Michael Kemp W. (2013). Sediment flux modeling: Calibration and application for coastal systems. *Estuarine, Coastal, and Shelf Science*. 117, 107-124. DOI: 10.1016/j.ecss.2012.11.003

Brooks A & Edgington D. (1994). Biogeochemical control of phosphorus cycling and primary production in Lake Michigan. *Limnology and Oceanography*. 39(4), 961-968. DOI: 10.4319/lo.1994.39.4.0961

Broman E, et al. (2021). Active DNRA and denitrification in oxic hypereutrophic waters. *Water Research*. 194, 116954. DOI: 10.1016/j.watres.2021.116954

Burgin A & Hamilton S. (2007). Have we overemphasized the role of denitrification in aquatic ecosystems? A review of nitrate removal pathways. *Frontiers in Ecology and the Environment*. 5(2), 89-96. DOI: 10.1890/1540-9295(2007)5[89:HWOTRO]2.0.CO;2

Carpenter S, Caracao N, Correll D, Howarth R, Sharpley A, Smith V. (1998). Nonpoint pollution of surface waters with phosphorus and nitrogen. *Ecological Applications*. 8(3), 559-586. DOI: 10.1890/1051-0761(1998)008[0559:NPOSWW]2.0.CO;2

Choppala G, Moon E, Bush R, Bolan N, Carroll N. (2018). Dissolution and redistribution of trace elements and nutrients during dredging of iron monosulfide enriched sediments. *Chemosphere*. 201, 380-387. DOI: 10.1016/j.chemosphere.2018.01.164

D'Elia C. (1987). Too much of a good thing: Nutrient enrichment of the Chesapeake Bay. *Environment Science and Policy for Sustainable Development*. 29(2), 6-11 & 30-33

Donald D, Bogard M, Finlay K, Leavitt P. (2011). Comparative effects of urea, ammonium, and nitrate on phytoplankton abundance, community composition, and toxicity in hypereutrophic freshwaters. *Limnology and Oceanography*. 56(6), 2161-2175. DOI:10.4319/lo.2011.56.6.2161

Garrels R & Christ C. (1965). *Solutions, Minerals, and Equilibria*. Published February 1965, Harper & Row Publishers, Inc. Croneis G, editor. LCCN: 65-12674

Glibert P, et al. (2016). Pluses and minuses of ammonium and nitrate uptake and assimilation by phytoplankton, with emphasis on nitrogen-enriched conditions. *Limnology and Oceanography*. 61, 165-197. DOI: 10.1002/lno.10203

Hall P & Aller R. (1992). Rapid, small-volume, flow injection analysis for $\Sigma CO_2$ and $NH_4^+$ in marine and freshwaters. *Limnology and Oceanography*. 37(2), 1113-1119. DOI: 10.4319/lo.1992.37.5.1113

Howell E, Chomicki K, Kaltenecker G. (2012). Patteerns in water quality on Canadian shores of Lake Ontario: Correspondence with proximity to land and level of urbanization. *Journal of Great Lakes Research*. 38(SUPPL.4), 32-46. DOI: 10.1016/j.jglr.2011.12.005

Huisman J, Codd G, Paerl H, Ibelings B, Verspagen J, Visser P. (2018). Cyanobacterial blooms. *Nature Reviews Microbiology*. 16(8), 471-483. DOI: 10.1038/s41579-018-0040-1

Jahnke R. (1988). A simple, reliable, and inexpensive pore-water sampler. *Limnology and Oceanography*. 33(3), 483-487. DOI: 10.4319/lo.1988.33.3.0483

Jørgensen B & Revsbech N. (1985). Diffusive boundary layers and the oxygen uptake of sediments and detritus. *Limnology and Oceanography*. 30(1), 111-122. DOI: 10.4319/lo.1985.30.1.0111

Kiani M, Tammeorg P, Niemistö J, Simojoki A, Tammeorg O. (2020). Internal phosphorus loading in a small shallow lake: Response after sediment removal. *Science of the Total Environment*. 725, 138279. DOI: 10.1016/j.scitotenv.2020.138279

de Klein J, Overbeek C, Jørgensen C, Veraart A. (2017). Effect of temperature on oxygen profiles and denitrification rates in freshwater sediments. *Wetlands*. 37, 975-983. DOI: 10.1007/s13157-017-0933-1

Hansen H & Koroleff F. (1999). “Determination of nutrients”. *Methods of Seawater Analysis, Third edition*. Published 1999, WILEY-VCH. Grasshoff K, Kremling K, Erhardt M, editors.

Lamers L, Smolders A, Roelofs, J. (2002). The restoration of fens in the Netherlands. *Hydrobiologia*. 478, 107-130. DOI: 10.1023/A:1021022529475

Larson J, et al. (2020). Phosphorus, nitrogen, and dissolved organic carbon fluxes from sediments in freshwater rivermouths entering Green Bay (Lake Michigan; USA). *Biogeochemistry*. 147, 179-197. DOI: 10.1007/s10533-020-00635-0

Liu C, et al. (2015). Use of multi-objective dredging for remediation of contaminated sediments: a case study of a typical heavily polluted confluence area in China. *Environmental Science and Pollution Research*. 22, 17839-17849. DOI: 10.1007/s11356-015-4978-5

Lohrer A & Wetz J. (2003) Dredged-induced nutrient release from sediments to the water column in a southeastern saltmarsh tidal creek. *Marine Pollution Bulletin*. 46, 1156-1163 DOI: 10.1016/S0025-326X(03)00167-X

Lomas M & Glibert P. (1999a). Interactions between $NH_4^+$ and $NO_3^-$ uptake and assimilation: Comparison of diatoms and dinoflagellates at several growth temperatures. *Marine Biology*. 133, 541-551. DOI: 10.1007/s002270050494

Lomas M & Glibert P. (1999b). Temperature regulation of nitrate uptake: A novel hypothesis about nitrate uptake and reduction in cool-water diatoms. *Limnology and Oceanography*. 44(3), 556-572. DOI: 10.4319/lo.1999.44.3.0556

Makarewicz J, et al. (2012a). Physical and chemical characteristics of the nearshore zone of Lake Ontario. *Journal of Great Lakes Research*. 38(SUPPL.4), 21-31. DOI: 10.1016/j.jglr.2011.11.013

Makarewicz J, Lewis T, Boyer G, Edwards W. (2012b). The influence of streams on nearshore water chemistry, Lake Ontario. *Journal of Great Lakes Research*. 38(SUPPL.4), 62-71. DOI: 10.1016/j.jglr.2012.02.010

Menounos B. (1997). The water content of lake sediments and its relationship to other physical parameters: an alpine case study. *The Holocene*. 7(2), 207-212. DOI: 10.1177/095968369700700208

Miller J. (1998). Confined disposal facilities on the great lakes. Published October 1998, United States Army Corps of Engineers.

Milwaukee Metropolitan Sewerage District (MMSD). “Dredged material management facility”. https://www.mmsd.com/what-we-do/milwaukee-estuary-aoc/dredged-material-management-facility. Accessed July 14, 2023.

Moncelon R, et al. (2021). Coupling between sediment biogeochemistry and phytoplankton development in a temperate freshwater marsh (Charente-Maritime, France): Evidence of temporal pattern. *Water Research*. 189, 116567. DOI: 10.1016/j.watres.2020.116567

Montenero M, Dilbone E, Waples J (2017). Using medically-derived iodine-131 to track sewage effluent in the Laurentian Great Lakes. *Water Research*. 123, 773-782. DOI: 10.1016/j.watres.2017.07.022

Nixon S. (1995). Coastal marine eutrophication: A definition, social causes, and future concerns. *Ophelia*. 41(1), 199-219.

Nogaro G & Burgin A. (2014). Influence of bioturbation on denitrification and dissimilatory nitrate reduction to ammonium (DNRA) in freshwater sediments. *Biogeochemistry*. 120, 279-294. DOI: 10.1007/s10533-014-9995-9

Pettersson K. (1998). Mechanisms for internal phosphorus loading in lakes. *Hydrobiologia*. 373/374, 21-25.

Reis E, Lodolo A, Miertus S. (2007). Survey of sediment remediation technologies. Published 2007, International Center for Science and High Technology.

Shen R, et al. The determining factors of sediment nutrient content and stoichiometry along profile depth in seasonal winter. (2023). *Science of the Total Environment*. 856, 158972. DOI: 10.1016/j.scitotenv.2022.158972

Smolders A, Lamers L, Lucassen E, Van der Velde G, Roelofs J. (2006). Internal eutrophication: How it works and what to do about it – a review. *Chemistry and Ecology*. 22(2), 93-111. DOI: 10.1016/j.ecss.2012.11.003

Sugimoto R, Sato T, Tominaga O. (2014). Using stable nitrogen isotopes to evaluate the relative importance of external and internal nitrogen loadings on phytoplankton production in a shallow lake (Lake Mikata, Japan). *Limnology and Oceanography*. 59(1), 37-47. DOI: 10.4319/10.2014.59.1.0037

Tramontalo J & Bohlen W. (1984). The nutrient and trace metal geochemistry of a dredge plume. *Estuarine, Coastal and Shelf Science*. 18, 385-401. DOI: 10.1016/0272-7714(84)90079-9

Turek K & Hoellein T. (2015). The invasive Asian clam (*Corbicula fluminea*) increases sediment denitrification and ammonium flux in 2 streams in the midwestern USA. *Freshwater Science*. 34(2), 472-484. DOI: 10.1086/680400

United States Army Corps of Engineers (USACE) & Environmental Protection Agency (USEPA). (2003). *Great Lakes confined disposal facilities*. Published April 2003. Tyloch J, project manager. Miller J, editor.

United States Environmental Protection Agency (USEPA). (1995). *Cleaning Up Contaminated Sediments: A Citizen's Guide.* Published 1995 by USEPA Great Lakes National Program Office, Assessment and Remediation of Contaminated Sediment (ARCS) Program. EPA 905/K-95/001.

United States Environmental Protection Agency (USEPA). (2019). "Recommended human health recreational ambient water quality criteria or swimming advisories for microcystins and cylindrospermopsin". 84 Federal Register 26413-26414, 2019-11814.

United States Environmental Protection Agency (USEPA). (2023). "Milwaukee estuary AOC". https://www.epa.gov/great-lakes-aocs/milwaukee-estuary-aoc. Accessed July 19, 2023

Ward B. (2013). "Nitrification". *Encyclopedia of Ecology*. 2nd ed. Published 2013, Elsevier. Fath B, editor. Pp 351-358. DOI: 10.1016/B978-0-12-409548-9.00697-7

Warnken K, Gill G, Dellapenna T, Lehman R, Harper D, Allison M. (2003). The effects of shrimp trawling on sediment oxygen consumption and the fluxes of trace metals and nutrients from estuarine environments. *Estuarine, Coastal and Shelf Science*. 57, 25-42 DOI: 10.1016/S0272-7714(02)00316-5

WEC Energy Group (2020) "Milwaukee Estuary AOC Dredged Material Management Facility", Project ID: 19W012. Published 2020 by WEC Energy Group – Business Services. Accessed August 15, 2023 via WDNR public records at https://dnr.wisconsin.gov/

Windom H. (1975). "Water quality aspects of dredging and dredge-spoil disposal in estuarine environments". *Estuarine Research, vol II: Geology and Engineering.* Cronin L E, editor.

Wisconsin Department of Natural Resources (WDNR). (2021). *Remedial action plan progress summary for the Milwaukee estuary area of concern*. Published August 2021. Dow B, editor.

Zadorojny C, Saxton S, Finger R. (1973). Spectrophotometric determination of ammonia. *Journal WPCF*. 45(5), 905-912.

Zappi P & Hayes D. (1991). *Innovative technologies for dredging contaminated sediments.* Pubilshed 1991 by USACE, U.S. Army Engineer Waterways Experiment Station.

Zhong J, Wen S, Zhang L, Wang J, Liu C, Yu J, Zhang L, Fan C. (2021). Nitrogen budget at sediment-water interface altered by sediment dredging and settling particles: Benefits and drawbacks in managing eutrophication. *Journal of Hazardous Materials*. 406, 124691. DOI: 10.1016/j.jhazmat.2020.124691

Zilius M, Daunys D, Petkuviene J, Bartoli M. (2021). Sediment-water oxygen, ammonium, and soluble reactive phosphorus fluxes in a turbid freshwater estuary (Curonian lagoon, Lithuania): evidences of benthic microalgal activity. *Journal of Limnology*. 71(2), 309-319. DOI: 10.4081/jlimnol.2012.e33

# APPENDICES

## Appendix A: Chloride, Sulfate, and Silicate Dynamics

Several analytes not directly relevant to the main content of this study were also analyzed where sample volumes permitted. These are part of the normal suite of chemical analyses done for work on the nutrient dynamics of Lake Michigan generally but were not prioritized here due to the focus placed on eutrophicating nutrients. Analytical results for these analytes are summarized below.

### Chloride

Within the Milwaukee estuary, chloride is a conservative element, meaning it is not subject to biogeochemical influences. This makes it useful as a control for the dilution of river water into the lake, making it possible to isolate only those changes in nutrients that are due to the biogeochemical processes of interest. Chloride is similarly conservative in sediments, its concentration in the porewater only changing when chloride either enters or escapes the sediment, for example via groundwater intrusion.

Chloride was only determined in surface porewaters for two sampling dates, 25 July, 2022 and 18 January, 2023. These data are shown in Figure 31. There is a clear increase in chloride between the two dates among all samples that were collected at both. This is likely the result of the application of road salt and salt brine in Milwaukee as de-icing measures during the winter months. The leaching dynamics of chloride are shown in Figure 32, where concentrations did not change significantly over time. This is likely due to the concentration of the porewater, diluted 1:10 into the receiving harbor water, being much lower than that already present in the receiving water.

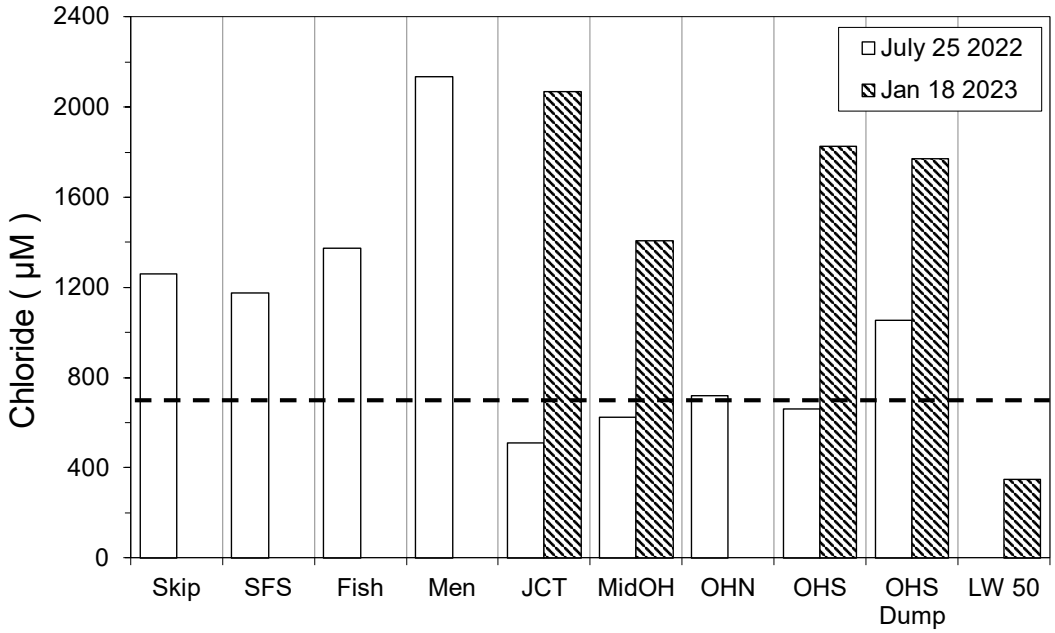


Figure 31: Chloride contents of surface sediment porewaters. The dashed line represents the typical chloride concentration of the outer harbor, usually between 600-800 µM.

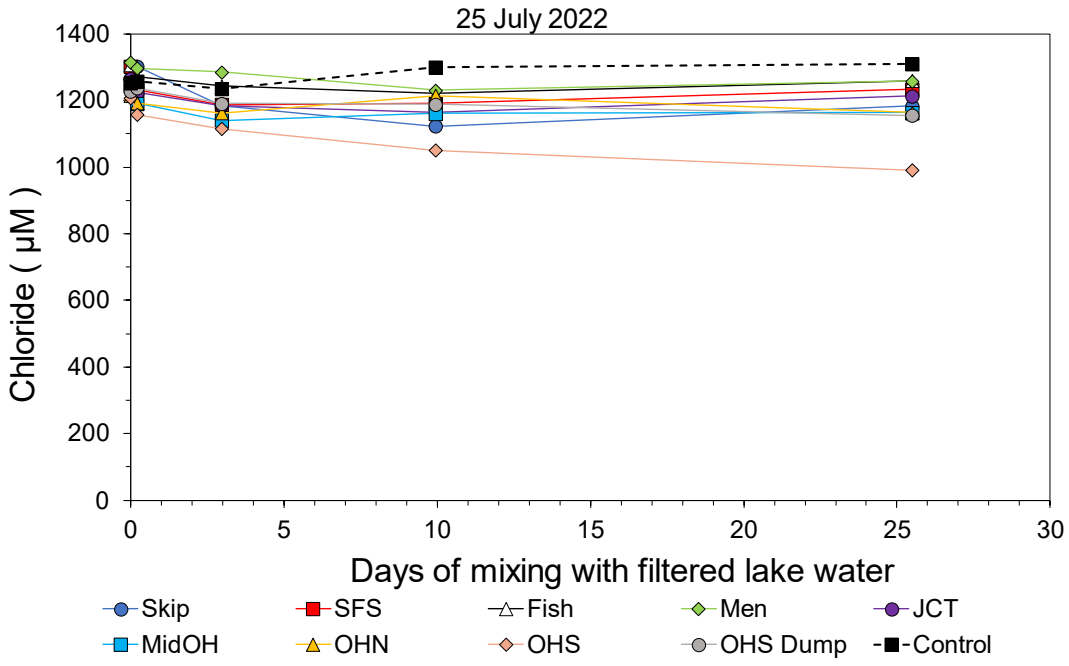


Figure 32: Chloride dynamics from the 25 July, 2022 leaching experiment.

**Sulfate**

Unlike chloride, sulfate is not conservative in Lake Michigan and is subject to biogeochemical processes. However, it is present in such excess relative to that required by the microbial population that it is almost never considered a eutrophicating nutrient. In the Milwaukee estuary, sulfate displays the unusual characteristic of remaining at a nearly constant concentration in the waters from the lower stretches of the rivers and out to Lake Michigan. This gives the illusion of sulfate not being subject to dilution at all.

Sulfate surface sediment porewater concentrations were highest at OHS by a significant margin, approximately 3-4 times higher than the next highest stations and 5-6 times higher than is normal for the estuary waters (Figure 33). All other stations had sulfate porewater contents at or below the normal water concentration. This is to be expected of surface sediments rich in organic material as decomposition depletes oxygen and anaerobic sulfur respiration begins, transforming sulfate ($SO_4^{2-}$) into sulfide and hydrogen sulfide ($S^{2-}$ and $H_2S$, respectively). As stated previously, this could explain the odor of the river sediment and porewater samples, and possibly may also have contributed to the positive error in the TAN analysis. However, this does little to explain why the OHS sediment samples were so highly enriched in sulfate.

Sulfate leaching dynamics were characterized by a sharp increase by $t_1$ followed by a more gradual increase through the remainder of the experiment (Figure 34). Already by $t_1$, all samples had a much higher sulfate concentration than expected of the dilution, possibly suggesting the generation of sulfate (Figure 35). As with the porewater concentrations, OHS had a considerably higher sulfate content by the end of the experiment than its counterparts. SKIP and MidOH were also noticeably elevated above the rest, but not to the same extent as OHS.

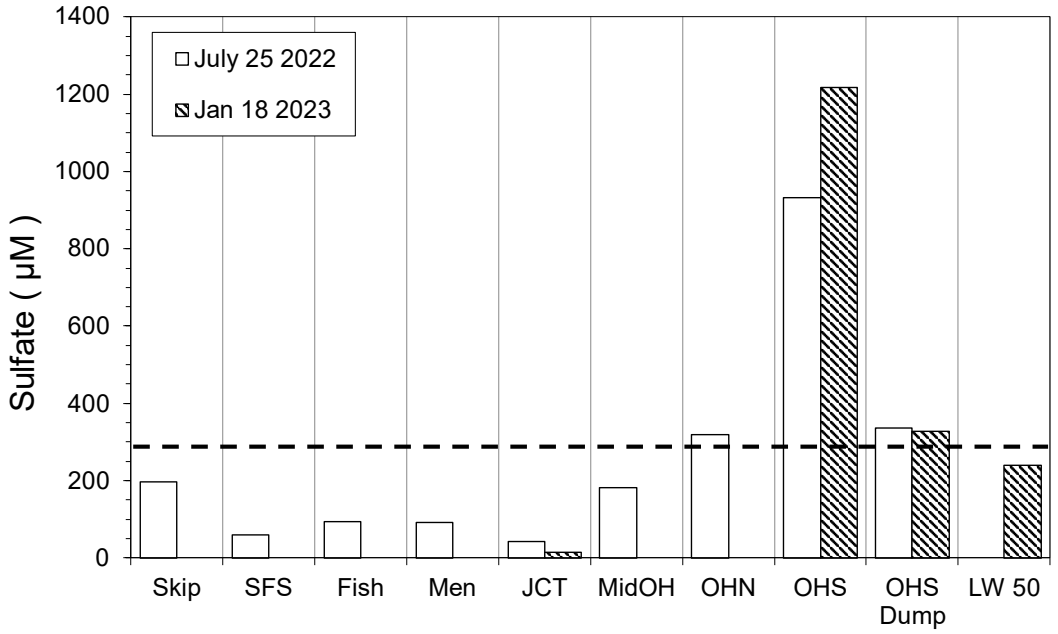


Figure 33: Sulfate contents of surface sediment porewaters. The dashed line represents the approximate sulfate concentration in the Milwaukee estuary, typically between 250-300 µM.

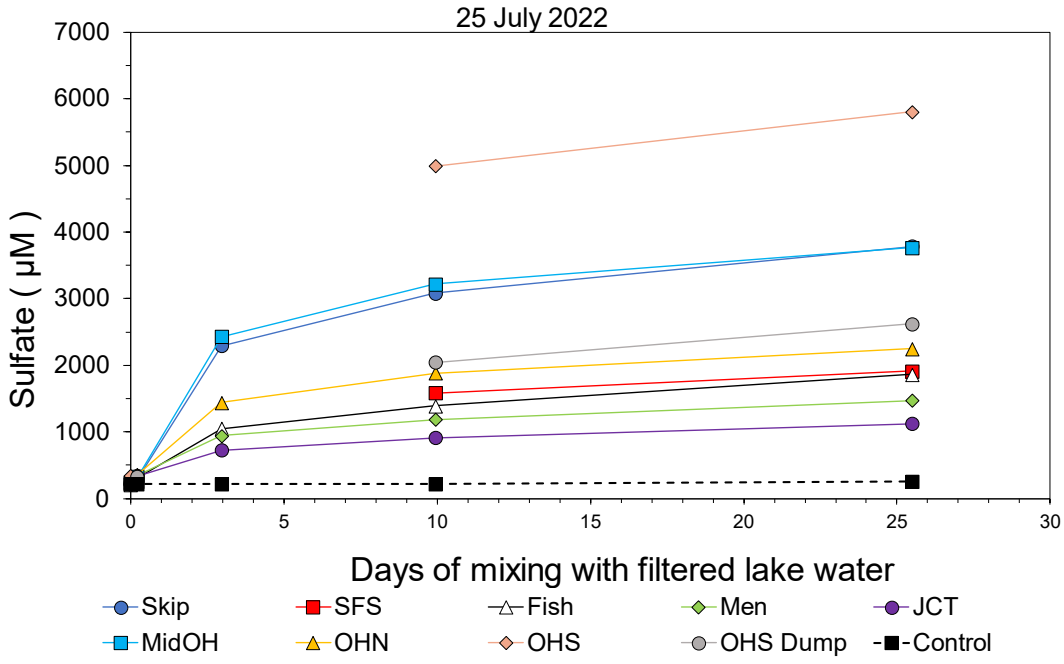


Figure 34: Sulfate dynamics from the 25 July, 2022 leaching experiment.

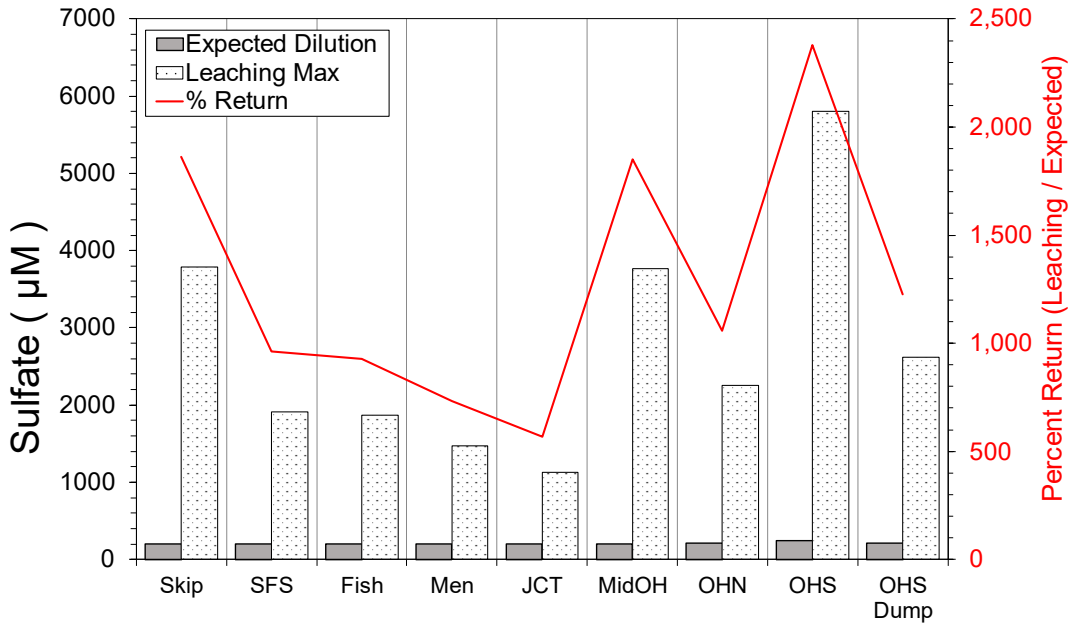


Figure 35: Observed vs. expected maximum sulfate leaching concentrations from the 25 July, 2022 leaching experiment.

**Dissolved Silicate**

Dissolved silicate (dSil) was measured for only four samples from 25 July, 2023, for the sole purpose of quickly testing whether the initial hypothesis that the porewater would be very highly elevated in dSil over the waters was true. It did indeed appear to be true, as the four samples measured were approximately 10 times higher in dSil than the waters (Figure 36). While dSil is an important nutrient for diatoms, as it is the material with which they develop their frustules, it is never a limiting nutrient for their growth in Lake Michigan due to being present in far higher concentrations than is typically required. It is likely that one source of dissolved silicate in porewaters is diatom diagenesis, accumulating dSil in sediments over time.

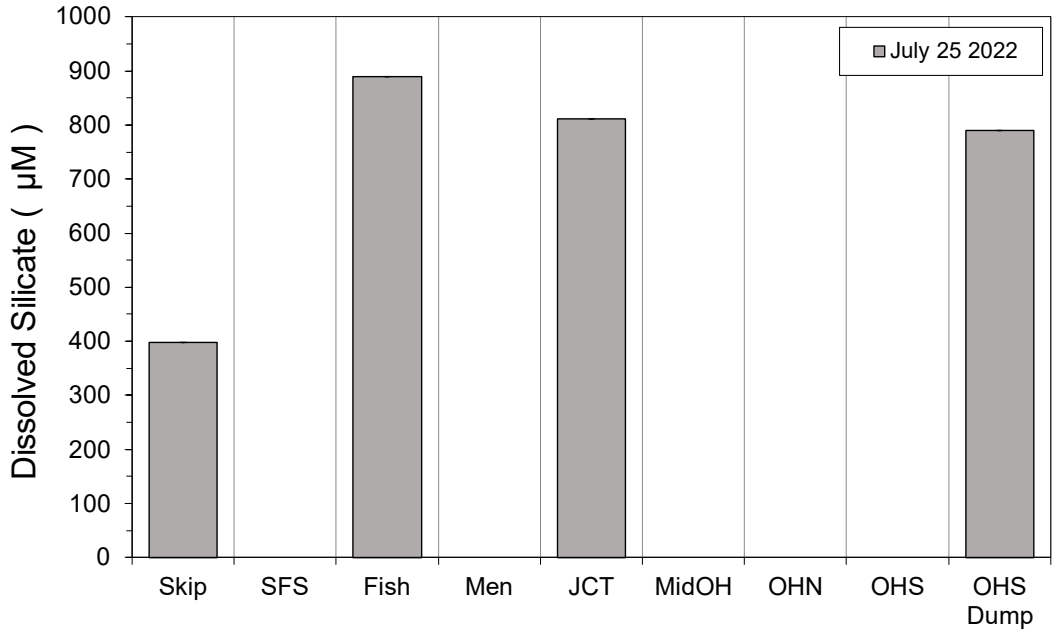


Figure 36: Dissolved silicate contents of select surface sediment porewater samples from 25 July, 2022.

## Appendix B: Sediment Metal Contents

Heavy metal remediation is one of the professed goals of the AOC dredging project. Additionally, many nutrient dynamics in aquatic environments can be coupled to metal dynamics. While metal dynamics were not the focus of this study, they were investigated for the 25 July, 2022 sample set. Those data are summarized in Table 2. All data are normalized by their water content, reflecting their content in a whole sediment sample (µmol metal per gram of whole sediment). The vast majority of metals present in sediment samples were in the solid fraction, though these could become dissolved if the waters above were to become acidified (by nitrification, perhaps). Of note is the fact that the porewater fraction (pore) and the solid fraction (pell, referring to the post-centrifugation pellet) do not add up to the whole sediment content (whole). This may indicate that some particulate- or colloidal- form metals are lost when the raw

porewater samples are filtered, suggesting that centrifugation does not partition all particles into the solid pellet, though this would not have affected the quantification of dissolved nutrients that was the focus of this study. Metals were determined by ICP-OES by Dr. John Ejnik, University of Wisconsin-Whitewater.

Table 2: Metal contents in whole sediment samples, organized by porewater fraction (pore), solid fraction (pell), and the whole sample (whole).

| | As (umol/g) | Se (umol/g) | Mo (umol/g) | Cr (umol/g) | Zn (umol/g) | P (umol/g) | Pb (umol/g) | Cd (umol/g) |
|---|---|---|---|---|---|---|---|---|
| Skip pore | -2.95E-05 | -9.25E-05 | -5.58E-06 | 2.85E-06 | 6.27E-04 | 1.77E-03 | 2.33E-06 | 1.42E-06 |
| SFS pore | -7.11E-05 | -7.89E-05 | -1.46E-05 | 1.36E-05 | 9.79E-04 | 2.15E-04 | -3.41E-07 | -5.04E-07 |
| Fish pore | -1.06E-04 | 7.14E-06 | -2.04E-05 | 2.23E-06 | 7.57E-05 | 1.21E-03 | 2.90E-06 | -1.94E-07 |
| Men pore | -2.14E-05 | -9.26E-05 | -1.86E-05 | 1.03E-05 | 4.35E-05 | 1.49E-03 | -1.81E-05 | -1.86E-07 |
| JCT pore | -4.93E-05 | -1.19E-04 | -1.08E-05 | -1.29E-05 | 1.48E-04 | 3.28E-04 | 1.39E-05 | 1.21E-06 |
| MidOH pore | 1.77E-05 | -1.00E-04 | 3.23E-06 | 4.76E-05 | 5.25E-05 | 8.80E-03 | -8.39E-06 | -5.04E-08 |
| OHN pore | -4.18E-05 | -1.07E-04 | -1.02E-05 | 3.66E-06 | 3.75E-05 | 7.32E-03 | -9.96E-06 | -8.42E-07 |
| OHS pore | 6.96E-05 | -5.40E-06 | 7.22E-07 | 5.46E-07 | 2.31E-04 | 7.33E-03 | 3.11E-07 | 1.77E-06 |
| OHS dump pore | -8.28E-05 | -1.49E-04 | -1.44E-05 | -5.20E-06 | 4.80E-05 | 2.42E-04 | -1.66E-05 | 8.02E-08 |
| Skip pell | 0.076 | 0.041 | 0.016 | 1.421 | 4.250 | 22.768 | 0.967 | 0.046 |
| SFS pell | 0.032 | 0.032 | 0.005 | 1.082 | 2.105 | 19.857 | 0.202 | 0.025 |
| Fish pell | 0.016 | 0.022 | 0.003 | 0.305 | 1.123 | 12.698 | 0.242 | 0.011 |
| Men pell | 0.019 | 0.021 | 0.004 | 0.446 | 1.558 | 19.820 | 0.103 | 0.019 |
| JCT pell | 0.018 | 0.023 | 0.004 | 0.383 | 1.303 | 17.291 | 0.092 | 0.014 |
| MidOH pell | 0.115 | 0.031 | 0.008 | 5.383 | 3.852 | 39.062 | 0.451 | 0.068 |
| OHN pell | 0.023 | 0.025 | 0.003 | 0.617 | 0.975 | 12.409 | 0.076 | 0.016 |
| OHS pell | 0.014 | 0.025 | 0.003 | 0.708 | 0.809 | 7.702 | 0.079 | 0.012 |
| OHS dump pell | 0.025 | 0.026 | 0.005 | 1.049 | 1.443 | 21.945 | 0.119 | 0.021 |
| Skip whole | 0.167 | 0.066 | 0.025 | 2.591 | 8.109 | 35.500 | 1.785 | 0.099 |
| SFS whole | 0.070 | 0.069 | 0.011 | 2.240 | 4.955 | 40.962 | 0.515 | 0.051 |
| Fish whole | 0.022 | 0.042 | 0.007 | 0.945 | 2.809 | 30.230 | 0.307 | 0.029 |
| Men whole | 0.038 | 0.047 | 0.010 | 0.897 | 3.182 | 35.976 | 0.221 | 0.036 |
| JCT whole | 0.038 | 0.044 | 0.007 | 0.995 | 3.579 | 41.591 | 0.224 | 0.037 |
| MidOH whole | 0.201 | 0.042 | 0.014 | 10.222 | 7.461 | 65.121 | 0.949 | 0.125 |
| OHN whole | 0.029 | 0.050 | 0.005 | 1.030 | 1.717 | 20.101 | 0.127 | 0.027 |
| OHS whole | 0.043 | 0.033 | 0.009 | 2.194 | 2.630 | 25.959 | 0.250 | 0.038 |
| OHS dump whole | 0.027 | 0.031 | 0.009 | 1.573 | 2.453 | 32.003 | 0.183 | 0.034 |

Table 2: (Continued) Metal contents in whole sediment samples, organized by porewater fraction (pore), solid fraction (pell), and the whole sample (whole).

| | Co (umol/g) | Ni (umol/g) | Mn (umol/g) | Fe (umol/g) | Mg (umol/g) | Al (umol/g) | Ca (umol/g) | Cu (umol/g) |
|---|---|---|---|---|---|---|---|---|
| Skip pore | 7.22E-06 | 1.07E-05 | 4.69E-03 | 2.60E-02 | 5.19E-01 | 3.50E-04 | 8.75E-01 | 1.58E-05 |
| SFS pore | 1.19E-05 | 8.84E-06 | 2.23E-02 | 6.53E-03 | 8.22E-01 | 3.79E-04 | 1.27E+00 | 2.37E-05 |
| Fish pore | 1.13E-05 | 1.75E-05 | 4.34E-02 | 5.06E-04 | 1.55E+00 | 2.80E-04 | 2.07E+00 | 2.34E-05 |
| Men pore | 1.17E-05 | -9.44E-08 | 4.82E-02 | 6.97E-03 | 1.04E+00 | 3.06E-04 | 1.58E+00 | 2.17E-05 |
| JCT pore | 3.19E-05 | 3.19E-05 | 4.61E-02 | 3.71E-03 | 1.59E+00 | 3.21E-04 | 2.75E+00 | 2.33E-05 |
| MidOH pore | 8.89E-06 | 2.33E-05 | 2.86E-03 | 8.06E-04 | 3.51E-01 | 3.33E-04 | 6.88E-01 | 1.90E-05 |
| OHN pore | 2.09E-06 | 4.75E-06 | 7.48E-03 | 1.63E-03 | 4.99E-01 | 2.31E-04 | 9.23E-01 | 2.03E-05 |
| OHS pore | 8.43E-06 | 1.03E-05 | 4.43E-03 | 4.72E-04 | 4.08E-01 | 3.97E-04 | 9.05E-01 | 1.79E-05 |
| OHS dump pore | 1.32E-05 | 1.28E-05 | 1.06E-02 | 1.03E-02 | 5.84E-01 | 2.84E-04 | 1.11E+00 | 2.18E-05 |
| Skip pell | 0.104 | 0.326 | 5.018 | 323.009 | 971.225 | 763.150 | 1208.807 | 0.872 |
| SFS pell | 0.063 | 0.168 | 5.486 | 240.525 | 575.881 | 487.678 | 862.997 | 0.613 |
| Fish pell | 0.041 | 0.082 | 4.432 | 128.044 | 545.244 | 226.538 | 992.007 | 0.396 |
| Men pell | 0.055 | 0.141 | 8.221 | 207.798 | 441.800 | 425.699 | 925.917 | 0.395 |
| JCT pell | 0.046 | 0.111 | 5.315 | 154.403 | 461.075 | 318.736 | 808.445 | 0.277 |
| MidOH pell | 0.067 | 0.282 | 4.124 | 201.255 | 862.704 | 372.287 | 1237.737 | 0.900 |
| OHN pell | 0.052 | 0.131 | 3.663 | 163.898 | 852.768 | 385.881 | 1156.967 | 0.411 |
| OHS pell | 0.037 | 0.100 | 2.146 | 117.601 | 411.538 | 296.402 | 1046.088 | 0.200 |
| OHS dump pell | 0.057 | 0.155 | 4.630 | 183.664 | 931.522 | 407.835 | 1299.941 | 0.376 |
| Skip whole | 0.182 | 0.571 | 7.611 | 512.422 | 1269.171 | 1296.605 | 1480.587 | 1.404 |
| SFS whole | 0.153 | 0.408 | 12.021 | 503.700 | 1336.360 | 1121.951 | 1994.313 | 1.067 |
| Fish whole | 0.106 | 0.241 | 13.035 | 309.585 | 1333.846 | 651.091 | 2416.190 | 0.599 |
| Men whole | 0.120 | 0.288 | 16.278 | 404.451 | 1197.823 | 861.407 | 2893.073 | 1.133 |
| JCT whole | 0.121 | 0.301 | 14.558 | 417.010 | 1374.502 | 913.112 | 2361.559 | 0.757 |
| MidOH whole | 0.120 | 0.547 | 7.958 | 357.059 | 1594.014 | 678.044 | 2272.237 | 1.768 |
| OHN whole | 0.098 | 0.245 | 7.501 | 322.443 | 1921.285 | 796.429 | 2513.639 | 0.469 |
| OHS whole | 0.122 | 0.328 | 7.735 | 360.655 | 1640.217 | 993.933 | 2242.246 | 0.641 |
| OHS dump whole | 0.102 | 0.265 | 9.505 | 320.727 | 1788.234 | 751.340 | 2484.245 | 0.624 |

Table 2: (Continued) Metal contents in whole sediment samples, organized by porewater fraction (pore), solid fraction (pell), and the whole sample (whole).

| | Ti (umol/g) | Sr (umol/g) | Ba (umol/g) | Na (umol/g) | Li (umol/g) | K (umol/g) |
|---|---|---|---|---|---|---|
| Skip pore | 1.82E-06 | 2.50E-03 | 1.02E-03 | 9.33E-01 | 3.50E-04 | 6.63E-02 |
| SFS pore | -8.25E-07 | 2.72E-03 | 2.18E-03 | 1.11E+00 | 3.23E-04 | 7.56E-02 |
| Fish pore | -7.01E-06 | 3.43E-03 | 1.84E-04 | 1.49E+00 | 3.62E-04 | 1.15E-01 |
| Men pore | 1.97E-07 | 2.71E-03 | 7.38E-05 | 1.67E+00 | 3.37E-04 | 7.06E-02 |
| JCT pore | -9.23E-06 | 5.24E-03 | 7.74E-04 | 1.16E+00 | 3.97E-04 | 1.28E-01 |
| MidOH pore | -1.04E-07 | 1.48E-03 | 8.14E-05 | 4.06E-01 | 2.26E-04 | 3.93E-02 |
| OHN pore | -4.20E-07 | 1.52E-03 | 7.71E-05 | 5.40E-01 | 2.38E-04 | 4.61E-02 |
| OHS pore | -1.90E-06 | 1.63E-03 | 2.19E-04 | 5.21E-01 | 2.32E-04 | 4.01E-02 |
| OHS dump pore | 5.68E-08 | 2.30E-03 | 1.03E-04 | 8.43E-01 | 3.26E-04 | 7.02E-02 |
| Skip pell | 5.349 | 0.795 | 0.936 | 12.011 | 3.069 | 155.187 |
| SFS pell | 4.024 | 0.464 | 0.651 | 10.975 | 2.010 | 90.835 |
| Fish pell | 2.620 | 0.408 | 0.386 | 8.402 | 0.853 | 37.067 |
| Men pell | 3.077 | 0.600 | 0.594 | 11.365 | 1.618 | 71.331 |
| JCT pell | 2.648 | 0.480 | 0.466 | 7.667 | 1.249 | 55.224 |
| MidOH pell | 4.300 | 0.499 | 0.828 | 10.886 | 1.507 | 68.605 |
| OHN pell | 3.038 | 0.365 | 0.418 | 10.342 | 1.638 | 77.672 |
| OHS pell | 2.556 | 0.669 | 0.379 | 11.361 | 1.220 | 59.369 |
| OHS dump pell | 3.448 | 0.433 | 0.510 | 7.486 | 1.664 | 80.314 |
| Skip whole | 9.718 | 1.300 | 1.597 | 25.595 | 5.355 | 254.874 |
| SFS whole | 7.701 | 1.078 | 1.484 | 25.711 | 4.286 | 209.085 |
| Fish whole | 6.728 | 1.190 | 1.094 | 21.820 | 2.474 | 106.776 |
| Men whole | 8.343 | 1.783 | 1.228 | 30.422 | 3.287 | 144.713 |
| JCT whole | 7.388 | 1.341 | 1.245 | 22.156 | 3.384 | 158.421 |
| MidOH whole | 7.614 | 0.889 | 1.451 | 20.187 | 2.694 | 117.919 |
| OHN whole | 7.156 | 0.723 | 0.780 | 20.806 | 3.353 | 164.478 |
| OHS whole | 7.041 | 0.843 | 1.044 | 21.949 | 4.169 | 202.158 |
| OHS dump whole | 7.474 | 0.807 | 0.875 | 20.484 | 3.104 | 145.242 |